Diastereoselective Synthesis of Aryl *C*-Glycosides via Radical Pathway

2024/1/11 (Thu) B4 Takashi Koyama

Outline

1. Introduction

2. Contents

    2-1. Homolytic activation of hydroxyl group and formation of radicals

    2-2. Stereoselective *C*-aryl glycosylation by catalytic cross-coupling of heteroaryl glycosyl sulfones

    2-3. Direct synthesis of unprotected aryl *C*-glycosides by photoredox Ni-catalysed cross-coupling

3. Summary

Conventional glycosyl donors (ionic pathway)

(a) *C*-Glycosylation via glycosyl electrophilic/cationic species

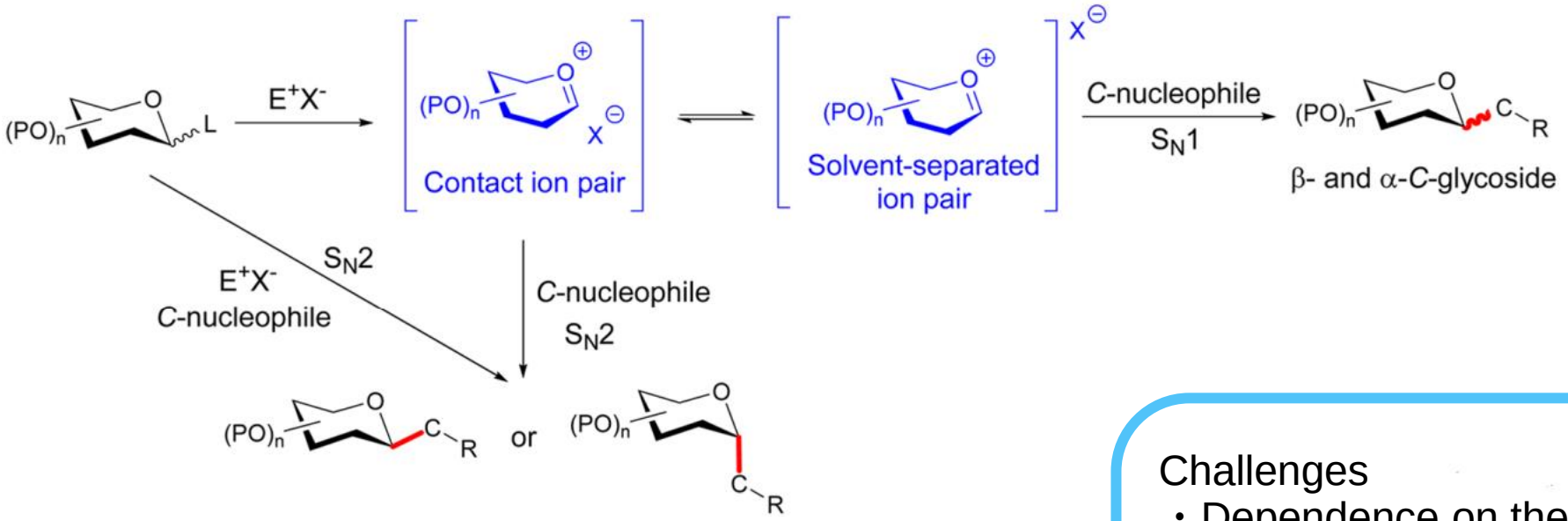

(b) *C*-Glycosylation via glycosyl anionic species

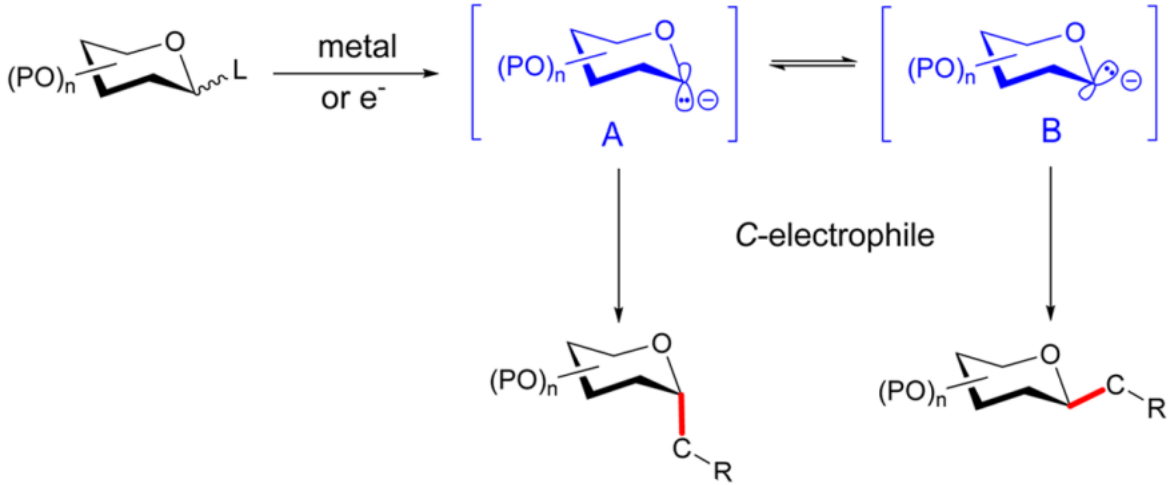

Challenges

- Dependence on the structures of donors/acceptors.
- Unstable glycosyl donors.
- Harsh reaction conditions.
- Incompatible with free hydroxyl group.
- Byproduct (ex. glycal, glycosidic bonds)
- Stereochemical purity of the glycosyl donors.

Y. Yang, B. Yu, *Chem. Rev*. **2017**, *117*, 12281–12356.

Reactive glycosyl intermediates

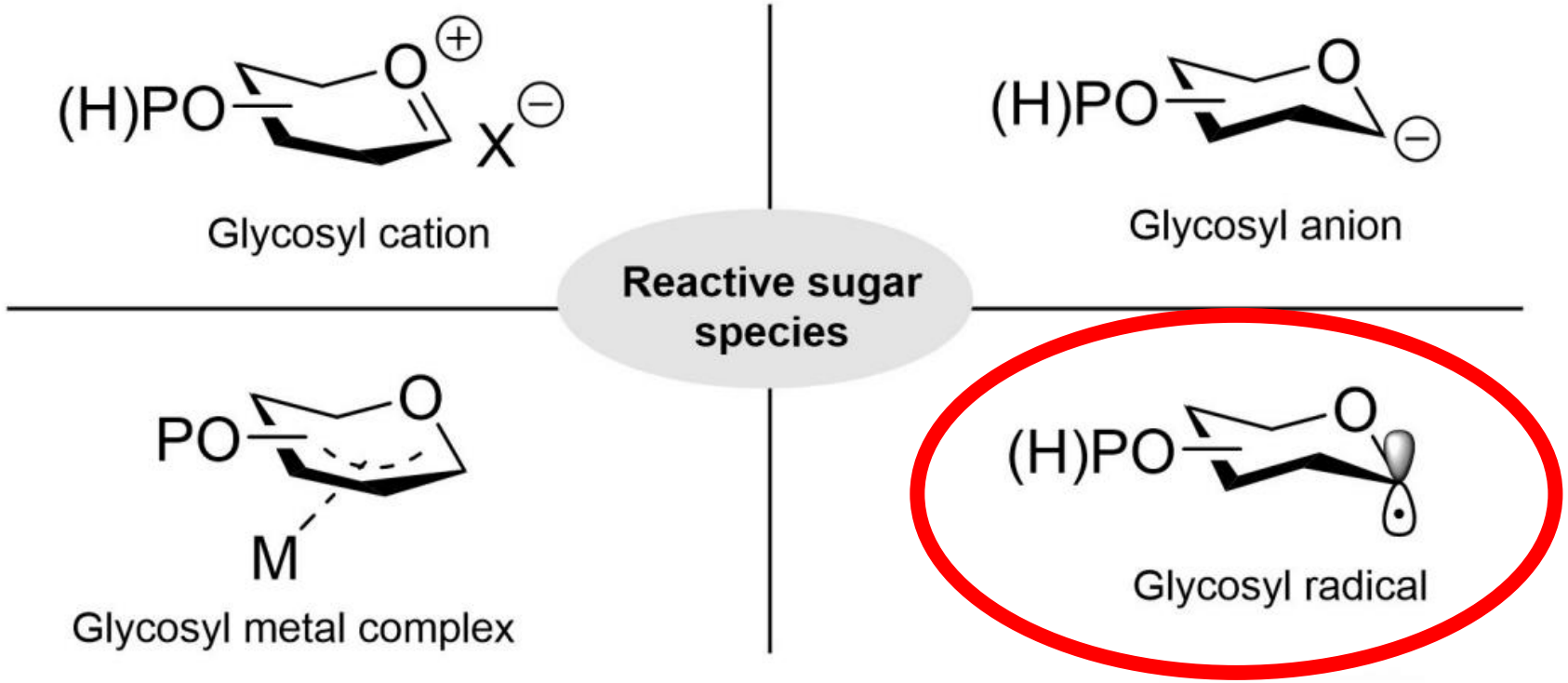

Regardless of the stereochemical purity of the glycosyl donors, both anomers will eventually converge to the sugar radical of the same conformation.

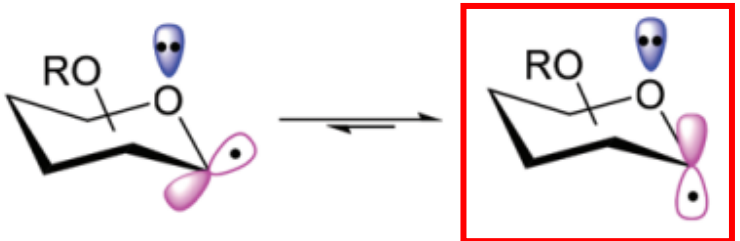

Y. Yang, B. Yu, *Chem. Rev*. **2017**, *117*, 12281–12356.
Y. jiang. et al. *Angew. Chem. Int. Ed*. **2023**, *62,* e202305138.

Factors determining stereoselectivity

① Anomeric effect

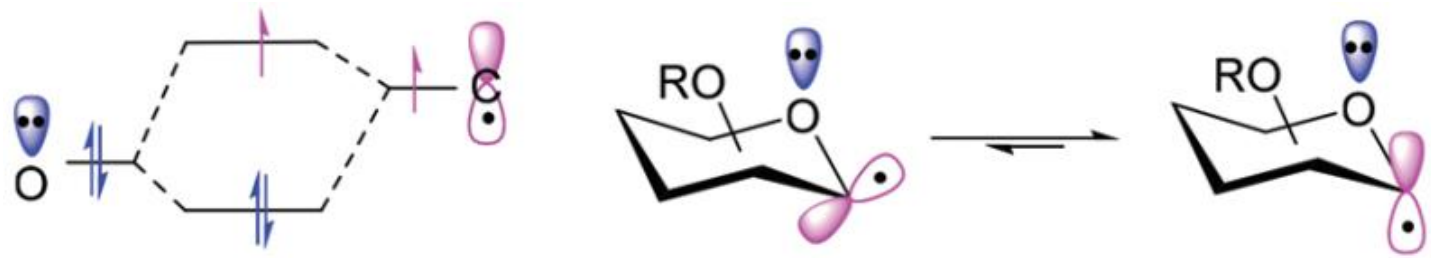

The axial radical is more stable and nucleophilic because of the interaction between the lone pair on the ring oxygen and the radical orbital.

② SOMO-LUMO interaction

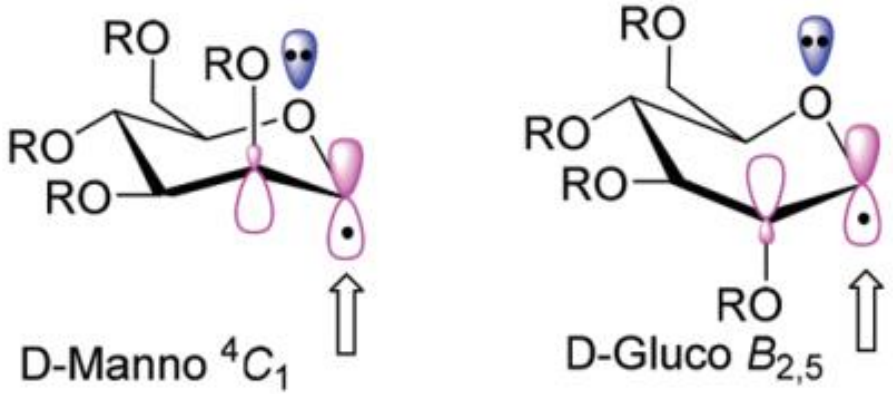

Stabilizing interaction between SOMO and LUMO of the neighboring C-O bond

H. Togo, W. He, Y. Waki, M. Yokoyama, *Synlett*, **1998**, 700–717.
Giese, B. *Angew. Chem. Int. Ed.* **1989**, **28**, 969–980.
H. Abe, S. Shuto, A. Matsuda, *J. Am. Chem. Soc*. **2001**, *123*, 11870.

Factors determining stereoselectivity

③ Conformation restriction

1

(2.70 kcal/mol)*

2

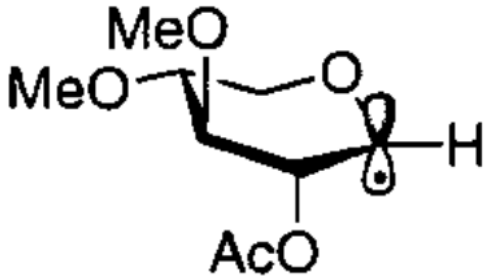

(0.94 kcal/mol)*

3

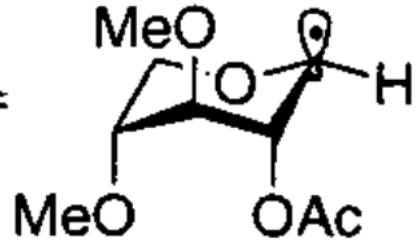

(0.00 kcal/mol)*

4

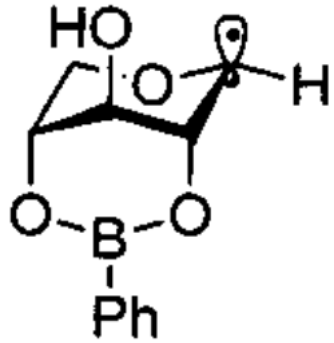

H. Abe, S. Shuto, A. Matsuda, *J. Am. Chem. Soc*. **2001**, *123*, 11870.
L. Y. Xu, N. L. Fan, X.-G. Hu, *Org. Biomol. Chem*. **2020**, *18*, 5095–5109.

5

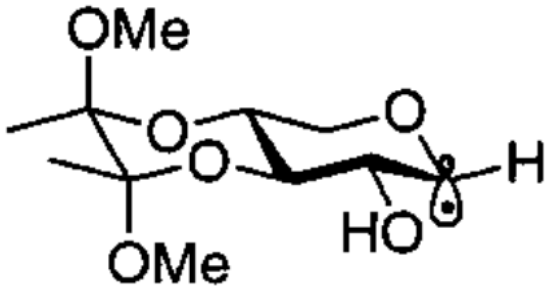

(0.00 kcal/mol)*

6

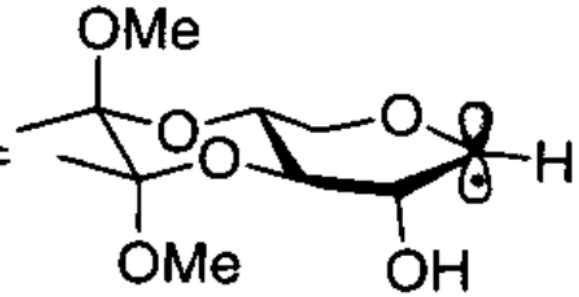

(3.55 kcal/mol)*

*relative energy

Conformational restriction of the pyranose ring changes the stereoselectivity in the anomeric radical reaction.

Factors determining stereoselectivity

④ Ligands effect in transition metal-catalyzed reactions

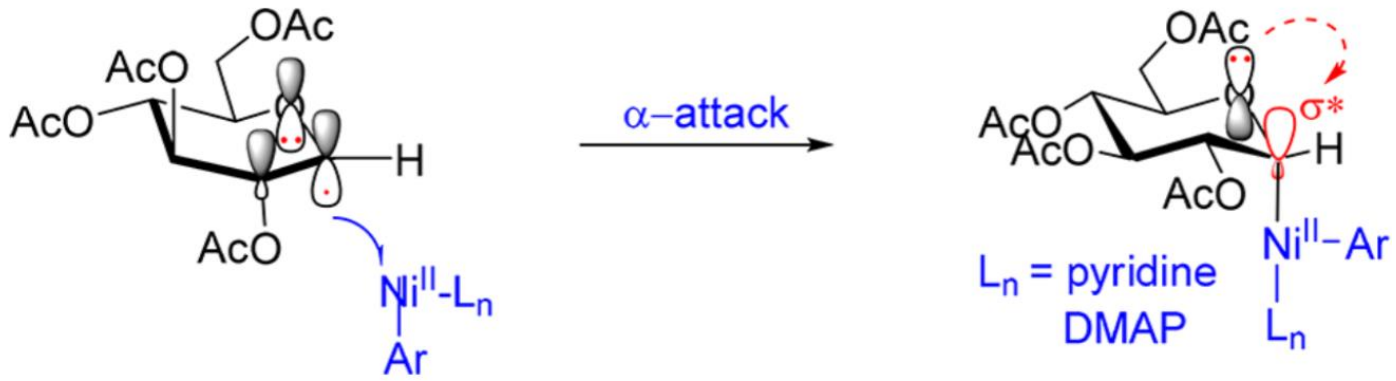

J. Liu, H. Gong, *Org Lett,* **2018**, *20,* 7991–7995.

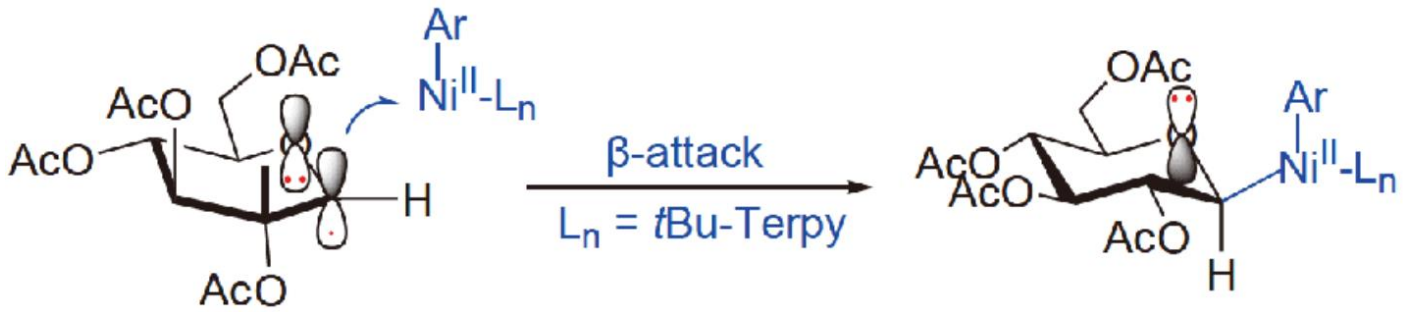

J. Liu, C. Lei, H. Gong, *Sci. China: Chem.,* **2019**, *62*, 1492–1496.

Bulky Ni-tridentate ligand complex seems to overcome the α-stereoselectivity

F. Zhu, M. A. Walczak, *J. Am.Chem.Soc*. **2020**,*142,*15127–15136.

Outline

1. Introduction

2. Contents

    2-1. Homolytic activation of hydroxyl group and formation of radicals

    2-2. Stereoselective *C*-aryl glycosylation by catalytic cross-coupling of heteroaryl glycosyl sulfones

    2-3. Direct synthesis of unprotected aryl *C*-glycosides by photoredox Ni-catalysed cross-coupling

3. Summary

Formation of carbon radicals from alcohols via C-O bond cleavage

(a) Homolytic activation of C-O bonds via redox-active groups

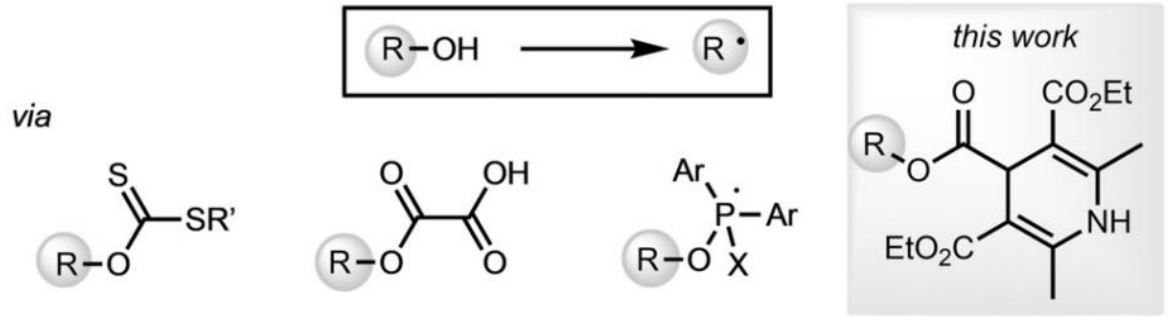

(b) Carbon radicals from aldehydes via C-C bond cleavage

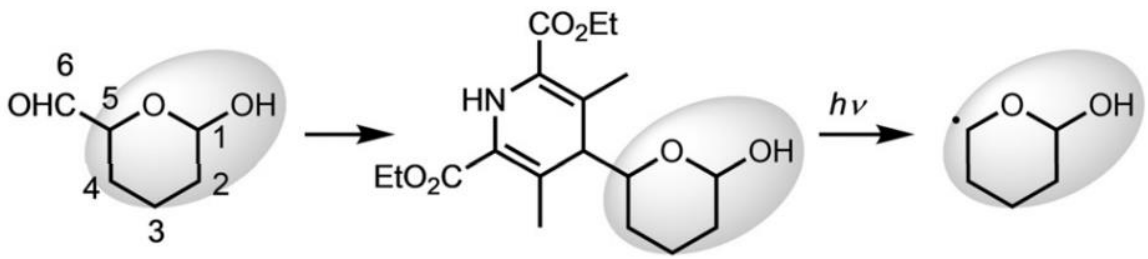

(c) Carbamoyl radicals from amines via C-C bond cleavage

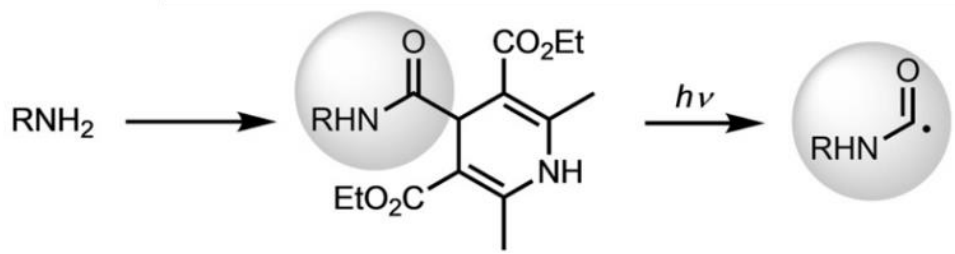

(d) Carbon radicals from alcohols via C-O bond cleavage

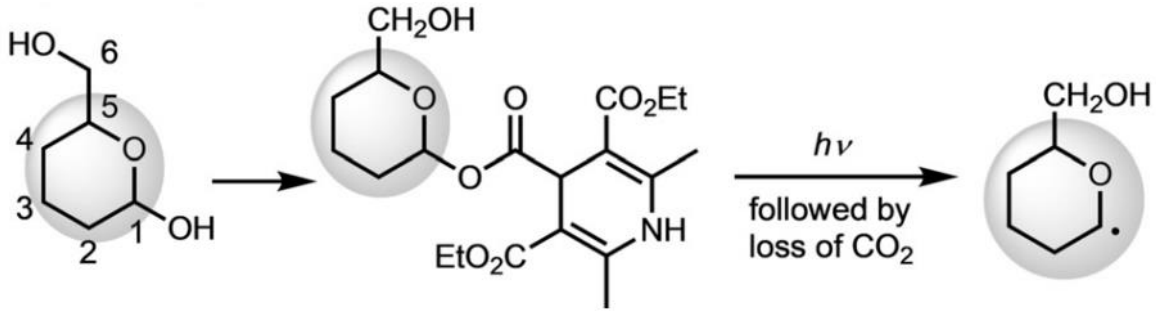

(a) Á. Gutiérrez-Bonet. *et al. ACS Catal*. **2016,** *6*, 8004.
(b) Á. Gutiérrez-Bonet. *et al*. *J. Am. Chem. Soc*. **2017**,*139*, 12251.
(c) N. Alandini. *et al. Angew. Chem. Int. Ed*. **2020**, *59,* 5248.
(d) Wei, Y., Ben-Zvi, B., Diao, T. *Angew. Chem. Int. Ed.* **2021**, *60*, 9433.

Proposed mechanism and optimized conditions

G. Ya. Dubur, Ya. R. Uldrikis, *Chem. Heterocycl. Compd*. **1972**, *5*, 762.

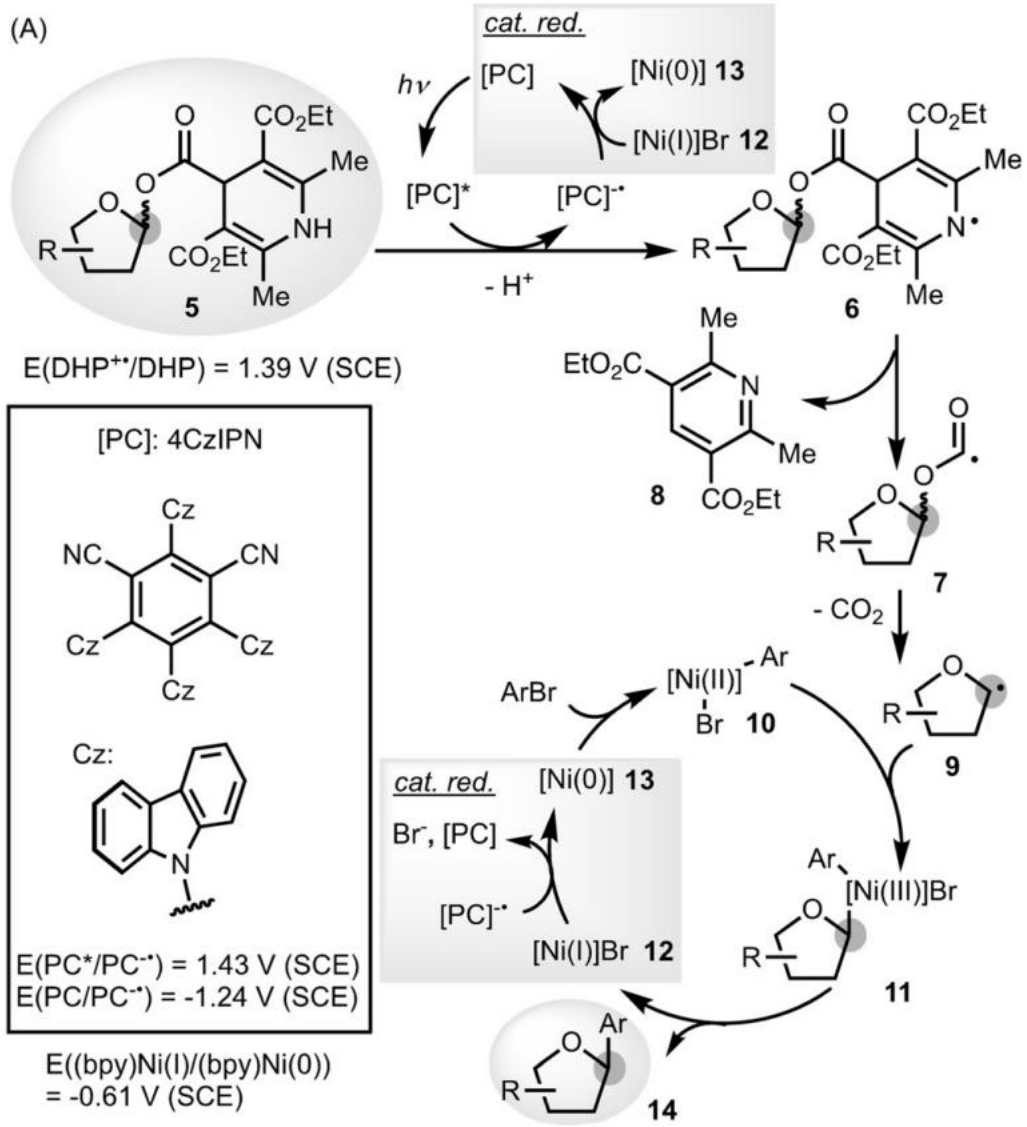

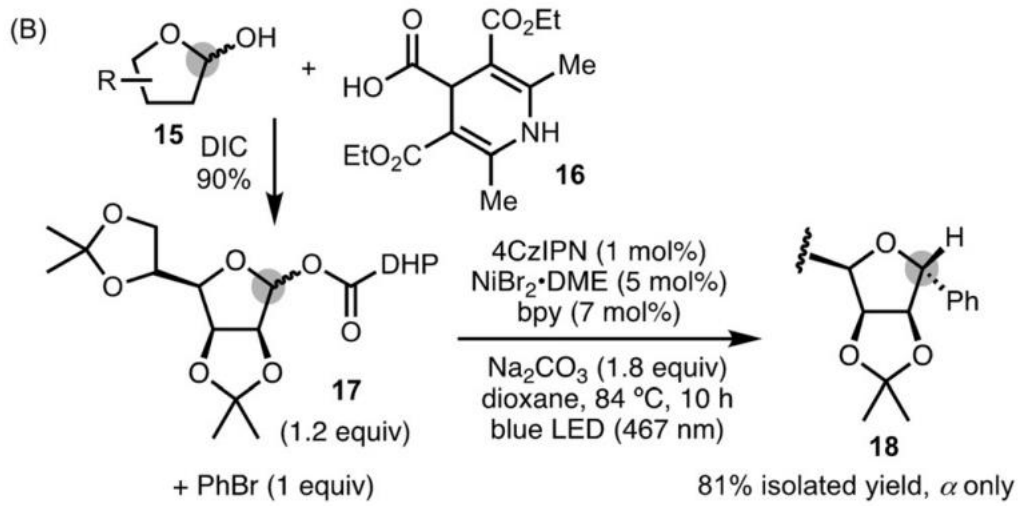

(A) Proposed mechanism for C-aryl glycosylation based on DHP derived estes
(B) Optimized conditions

- High temperature is required to facilitate DHP fragmentation and the subsequent decarboxylation.
- High α-selectivity because of C2, C3 and C4 substituents

Wei, Y., Ben-Zvi, B., Diao, T. *Angew. Chem. Int. Ed.* **2021**, *60*, 9433.

Substrate scope

Electrophiles

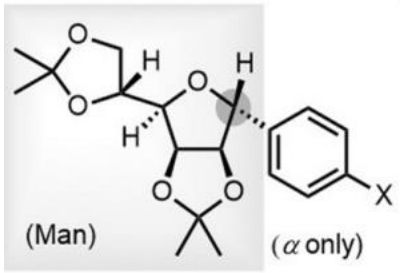

X = CN	**19**	82%
CF_3	**20**	90%
CO_2Me	**21**	92%
		82%[b]
Cl	**22**	74%
F	**23**	83%
H	**18**	81%
Me	**24**	61%
OMe	**25**	80%
NMe_2	**26**	<10%

D-mannofuranose

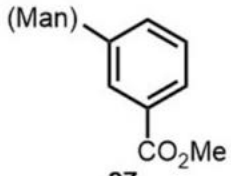

27
73% (α only) (73 °C)

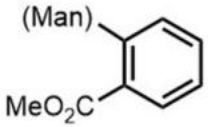

28
67% (α only)

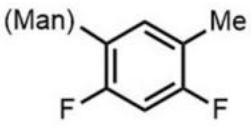

29
82% (α only)

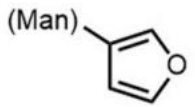

30
no reaction

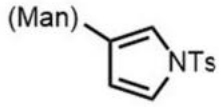

31
< 5%

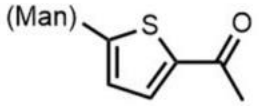

32
42% (α only) (90 °C)

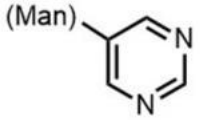

33
39%,[c] (α only) (90 °C)

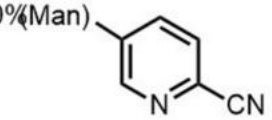

34
52% (α only)

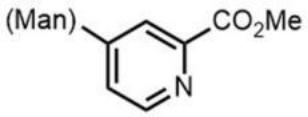

35
59% (α only) (90 °C)

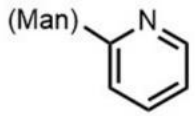

36
23%[d] (α only)

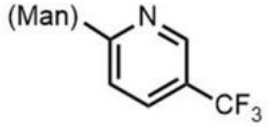

37
50%[c] (α only) (90 °C)

- Performing the synthesis of **17** on a 1.94-gramscale afforded **21** in 82% isolated yield.
- A lower temperature led to the formation of a byproduct derived from the coupling of **7** to PhBr.

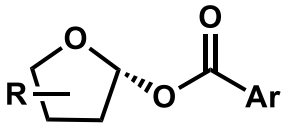

Wei, Y., Ben-Zvi, B., Diao, T. *Angew. Chem. Int. Ed.* **2021**, *60*, 9433.

Stereoselectivity

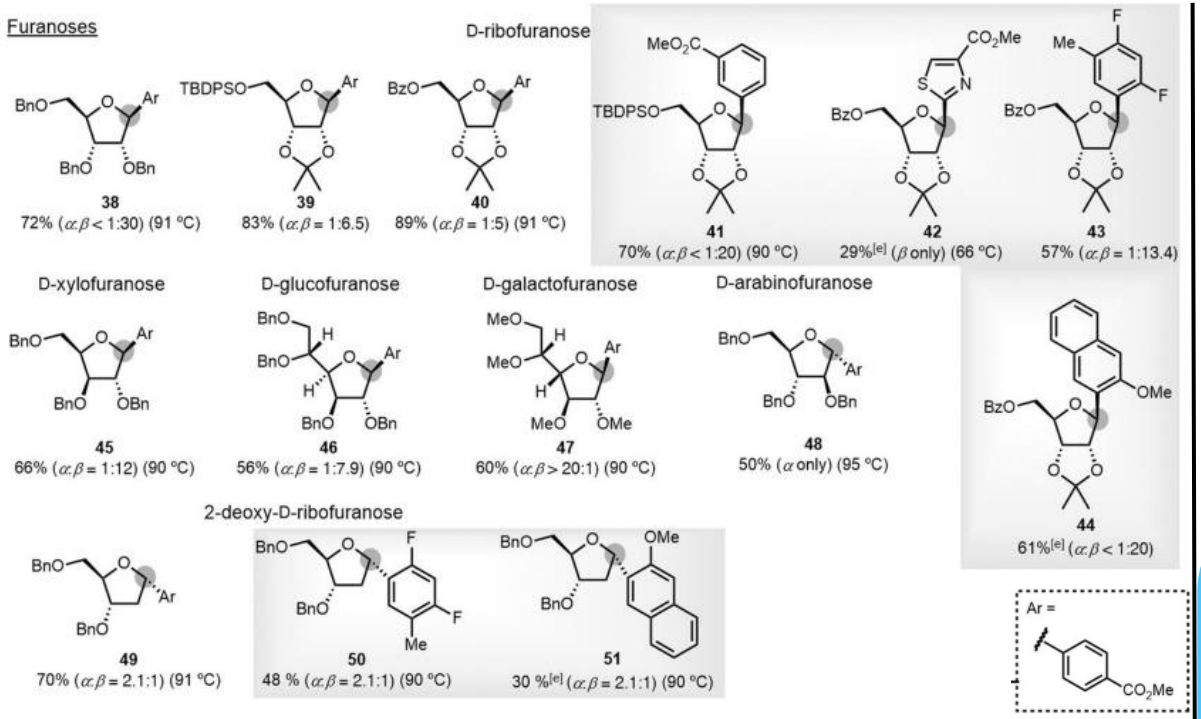

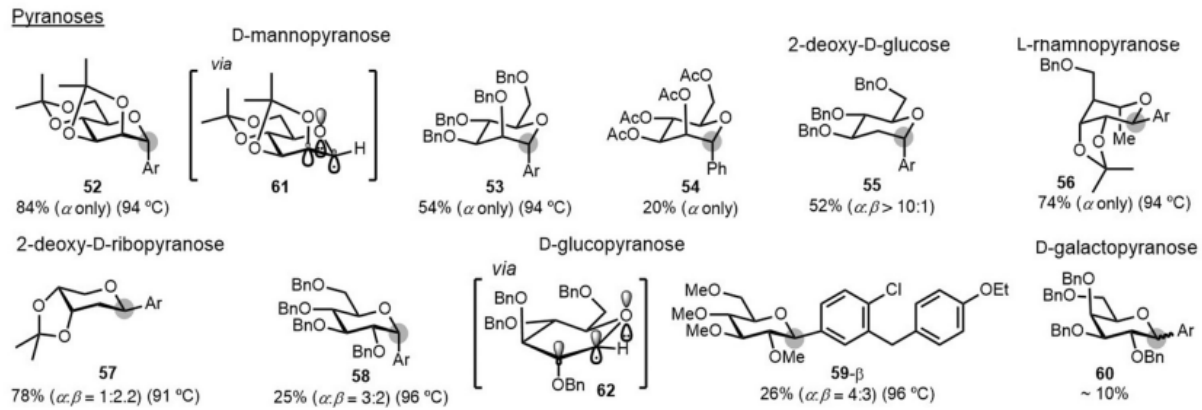

- Mannopyranoses display α-selectivity.
- Glucopyranoses display poor reactivity and stereoselectivity.
- The poor selectivity can be attributed to the contradictory preferences by the steric and the stereoelectronic effect.

Derivatization of (+)-sclareolide from deoxygenative cross coupling

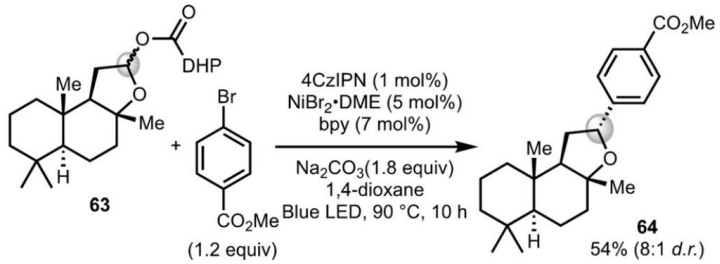

Wei, Y., Ben-Zvi, B., Diao, T. *Angew. Chem. Int. Ed.* **2021**, *60*, 9433.

Factor causing poor stereoselectivity of glucopyranoside

J. Dupuis, et al. *Angew. Chem. Int. Ed,* **1984,** *23*, 896–898.
H. Abe, S. Shuto, A. Matsuda, *J. Am. Chem. Soc*. **2001**, *123*, 11870.
H. Togo, W. He, Y. Waki, M. Yokoyama, *Synlett*, **1998**, 700–717.

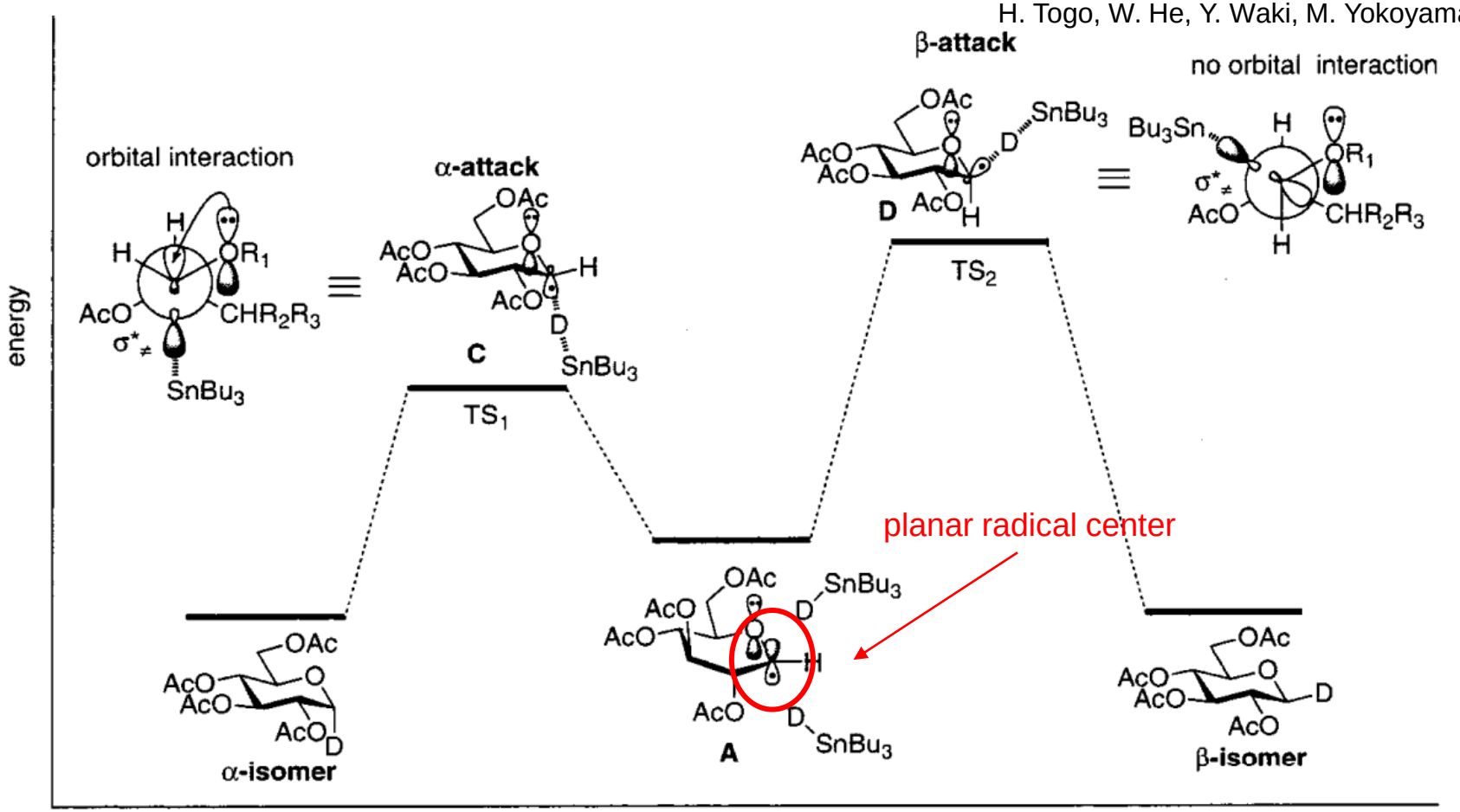

- $B_{2,5}$ conformation has a planar (sp^2-like) radical center with a radical orbital having high p-character.
- $B_{2,5}$ conformation has potential to form both anomers through α- and β- attack.
- In the transition state the radical center has more pyramidal (sp^3-like) radical center.

Factor causing poor stereoselectivity of glucopyranoside

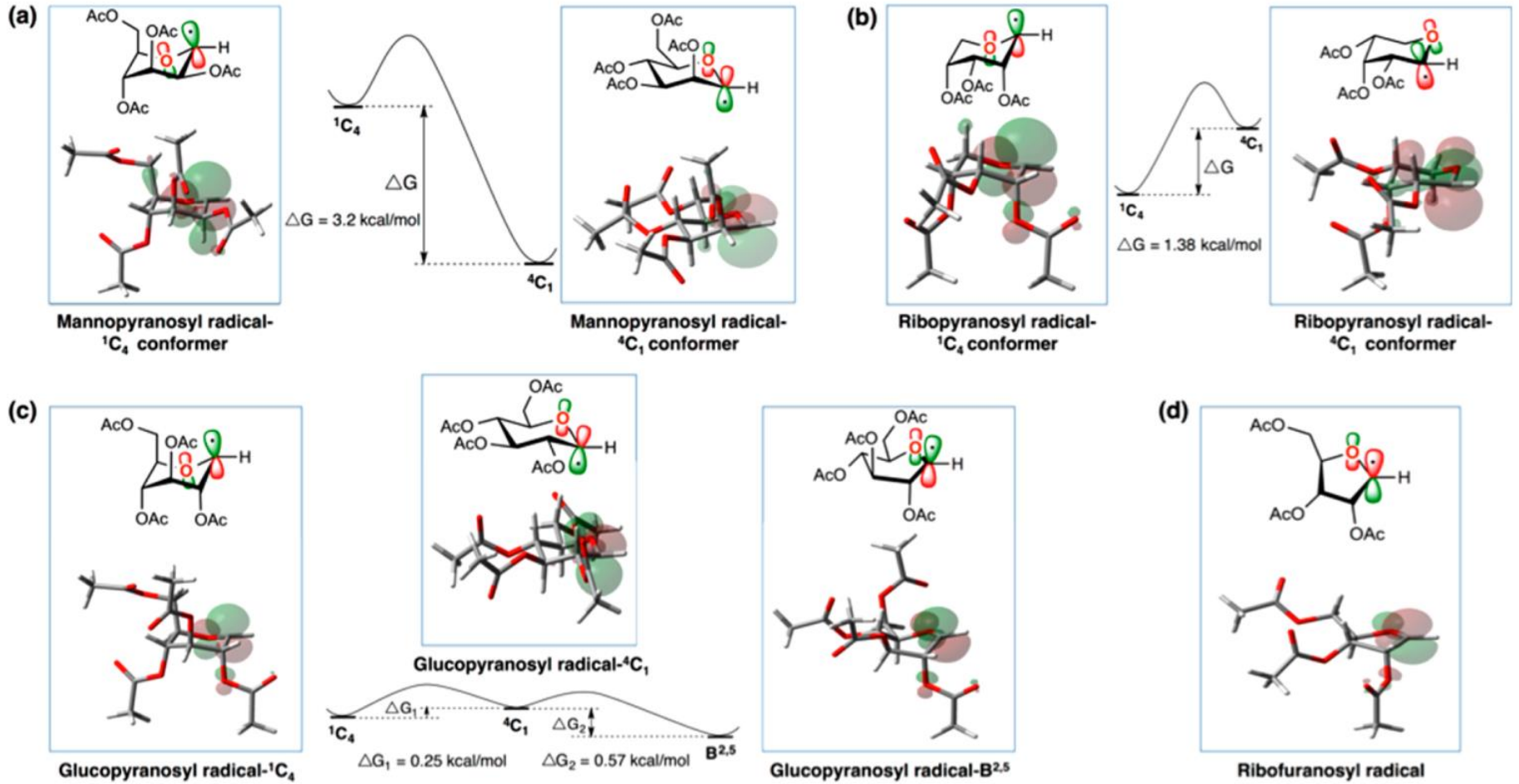

- Fluctuating conformational changes of the glucosyl radical leads to varied α/β selectivity.
- Contradictory preferences by the steric and the stereoelectronic effect are the factor of fluctuating conformational changes.

Adak, L. et al. *J. Am. Chem. Soc.* **2017**, *139*, 10693–10701.

Short summary

Homolytic activation of hydroxyl group and formation of radicals

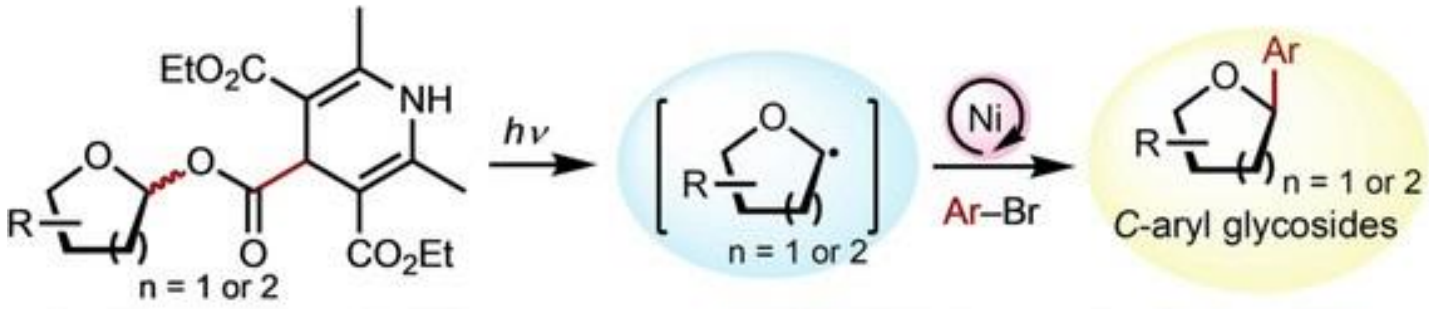

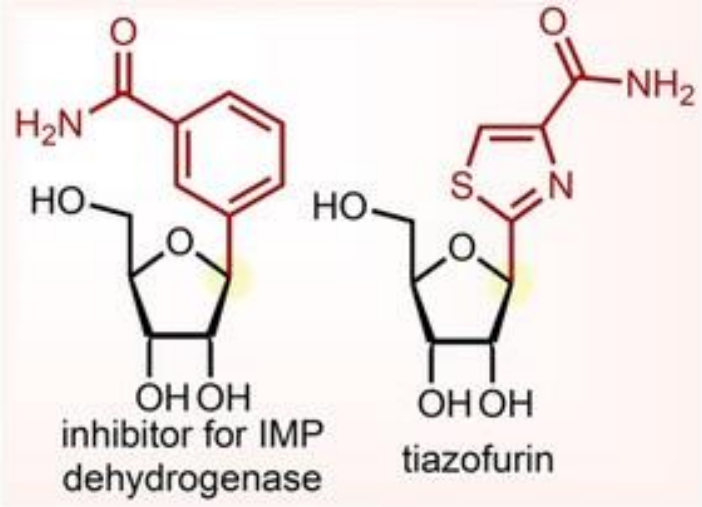

- ✓ Bench-stable.
- ✓ Easily accessible.
- ✓ Diastereoselective in furanoside.

- × Stereoselectivity of glucopyranose.
- × Protection of the hydroxyl groups.
- × High temperature.

Wei, Y., Ben-Zvi, B., Diao, T. *Angew. Chem. Int. Ed.* **2021**, *60*, 9433.

Outline

1. Introduction

2. Contents

    2-1. Homolytic activation of hydroxyl group and formation of radicals

    2-2. Stereoselective *C*-aryl glycosylation by catalytic cross-coupling of heteroaryl glycosyl sulfones

    2-3. Direct synthesis of unprotected aryl *C*-glycosides by photoredox Ni-catalysed cross-coupling

3. Summary

Heteroaryl glycosyl sulfones as practical donors for *C*-aryl glycosylation

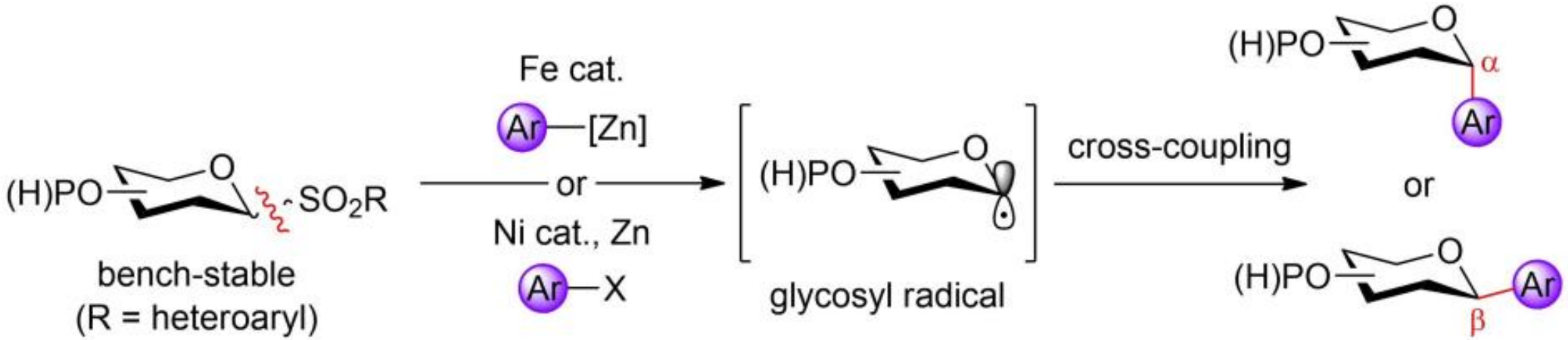

- broad sugar scope
- Ar nucleophiles & electrophiles
- distinct mechanisms and activation modes
- access to both α & β isomers for key sugars

Potential challenge:

Q. Wang, *et al. Angew. Chem. Int. Ed*. **2023**, *62,* e202301081.
J. Corpas, *et al. Chem. Soc. Rev.* **2022**, *51*, 6774–6823.

Optimized conditions

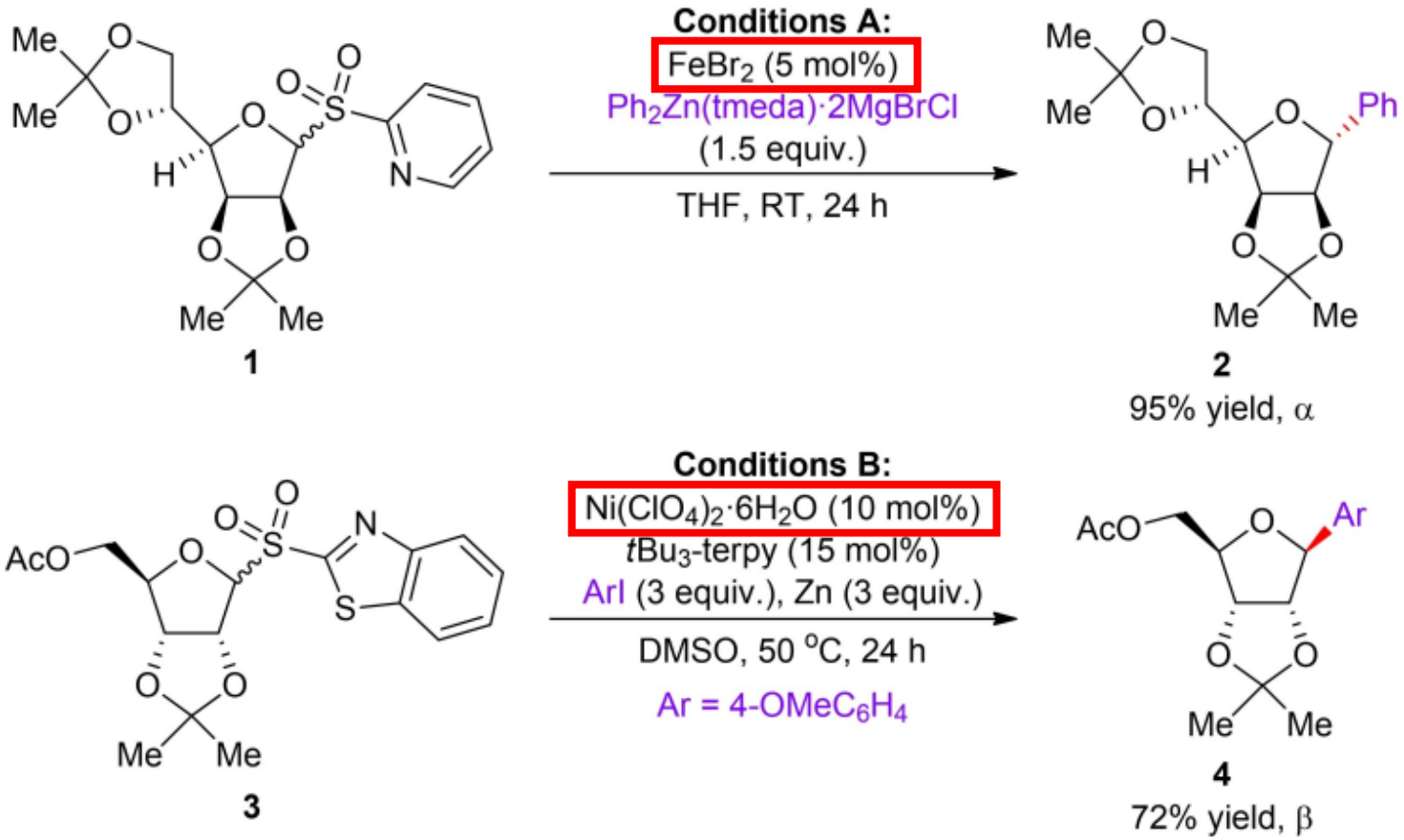

Conditions A

- The reactions proceed under room temperature.
- 2-Pyridyl sulfinate salt was detected as a byproduct.

Conditions B

- Benzothiazole and 2,2-bibenzothiazole were detected.

W. Miao. et al. *J. Am. Chem. Soc.* **2018,** *140*, 880–883.

Mechanistic studies

a. Radical trap experiment in Fe-catalyzed arylation

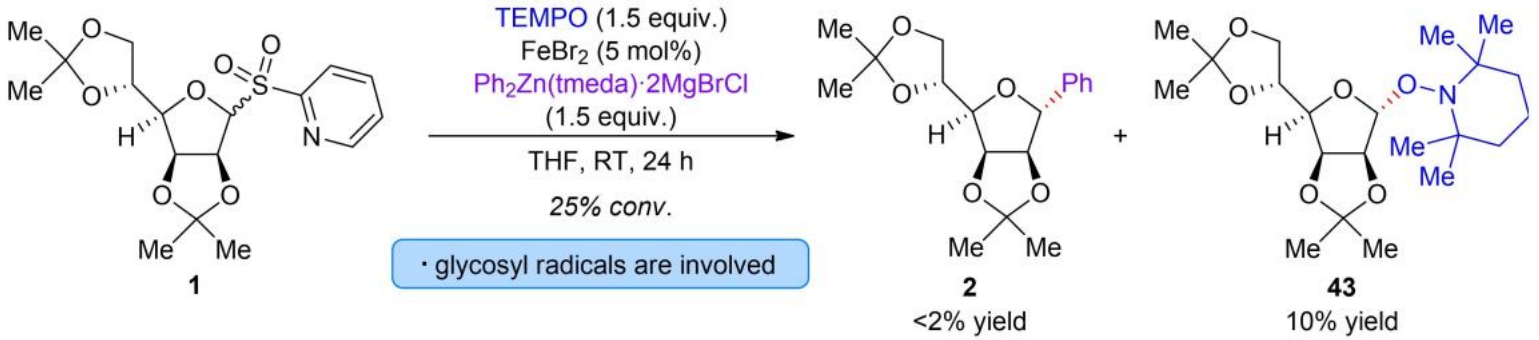

b. Radical trap experiments in Ni-catalyzed arylation and the role of Zn

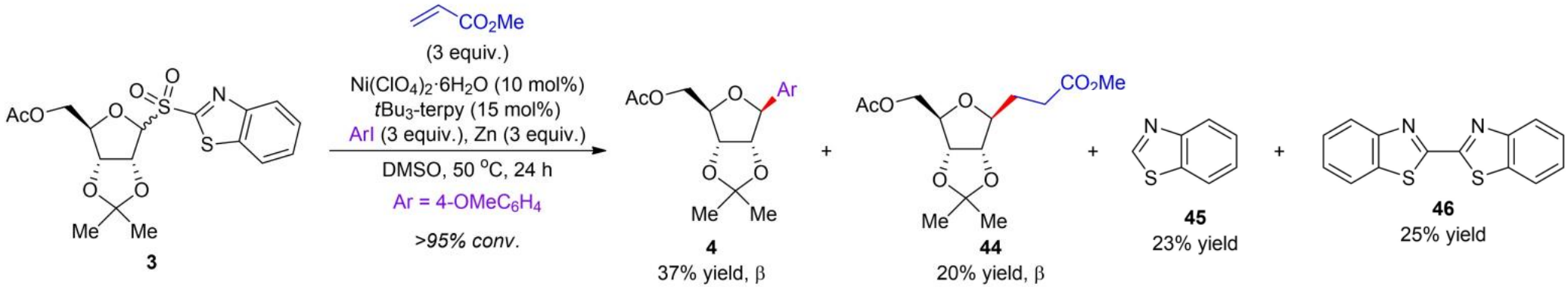

· glycosyl radicals are involved
· Zn can reduce sulfones

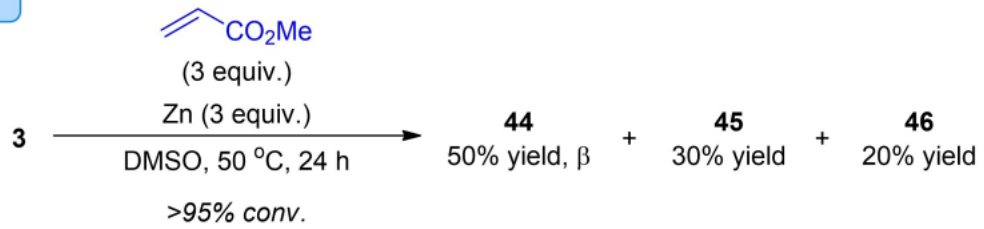

Q. Wang, *et al. Angew. Chem. Int. Ed*. **2023**, *62,* e202301081.

Proposed mechanisms for Fe- and Ni-catalyzed *C*-aryl glycosylation

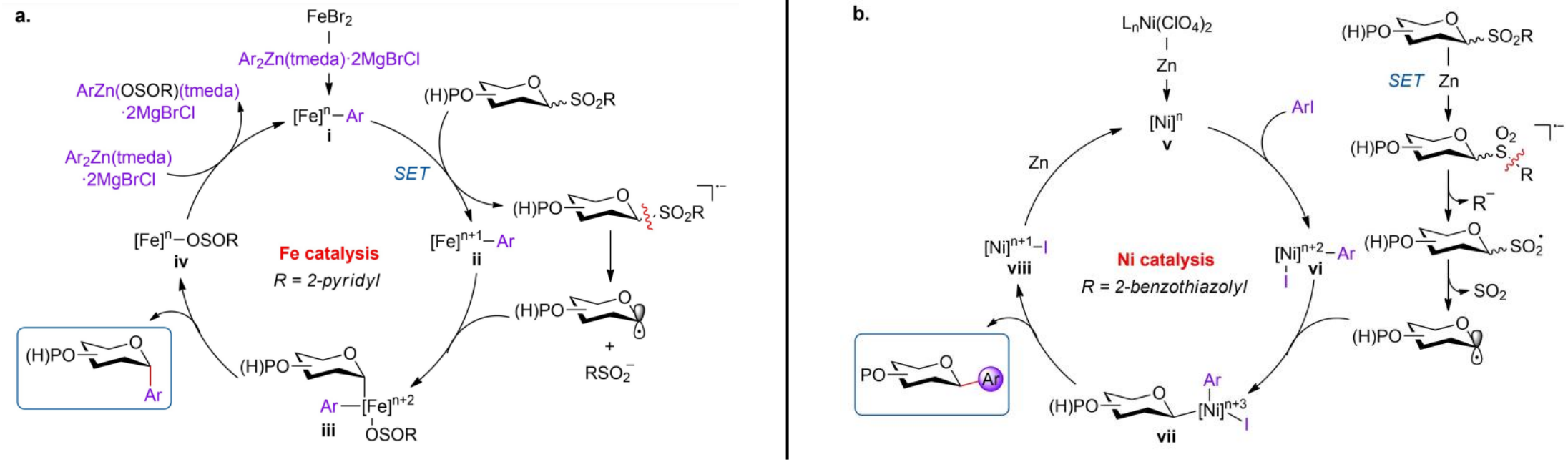

a.

- Aryl iron species **i** could serve as a reducing agent by SET to the electrophilic heteroaryl sulfone.
- Radical anion undergoes direct S-C(glycosyl) bond cleavage to form glycosyl radical and sulfinate.

W. Miao, *et al. J. Am. Chem. Soc.* **2018**, *140*, 880–883.

b.

- Zn could serve as a reducing agent by SET to the more electrophilic heteroaryl sulfone.
- Radical anion undergoes S-C(2-benzothiazoyl) bond cleavage to give glycosylsulfonyl radical and 2-benzothiazoyl anion.

J. M. E. Hughes, P. S. Fier, *Org. Lett*. **2019**, *21*, 5650–5654.

Fe-catalyzed desulfonylative arylation with diaryl zinc reagents

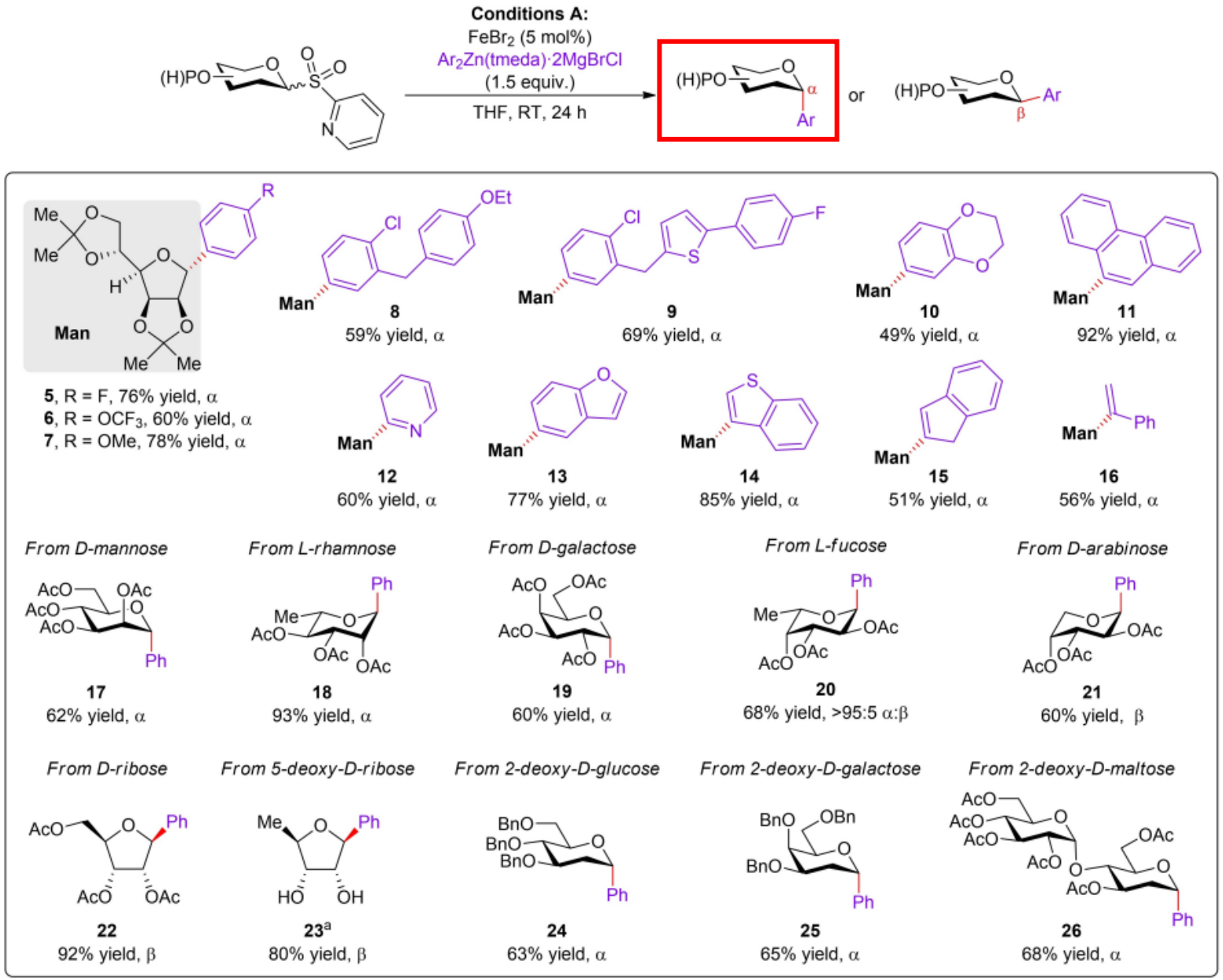

Ni-catalyzed desulfonylative arylation with aryl iodides

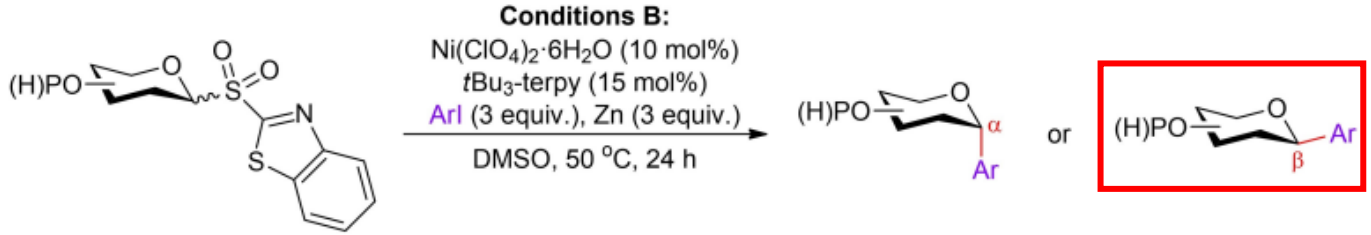

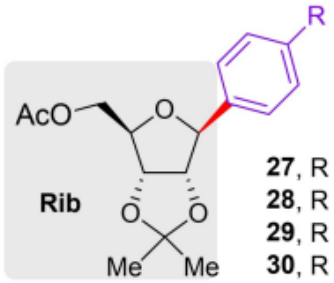

27, R = CN, 63% yield, β
28, R = Cl, 77% yield, β
29, R = CO_2Me, 71% yield, β
30, R = CH_2OAc, 80% yield, β

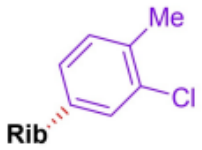

31
76% yield, β

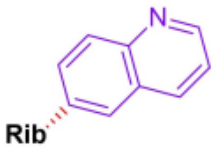

32
76% yield, β

33
85% yield, β

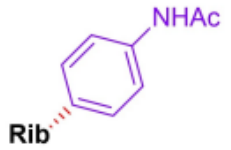

34
86% yield, β
(intermediate of β-RFAP)

From D-xylose

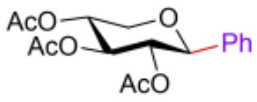

35
83% yield, β

From D-glucosamine

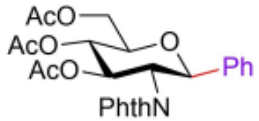

36
61% yield, β

From L-fucose

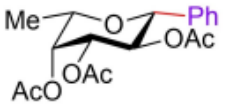

37
64% yield, β

From D-arabinose

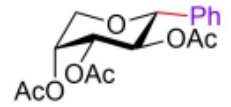

38
62% yield, 80:20 α:β

From D-galactose

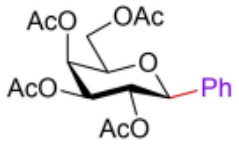

39
64% yield, β

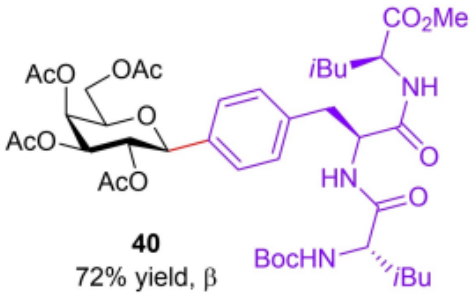

40
72% yield, β

From D-ribose

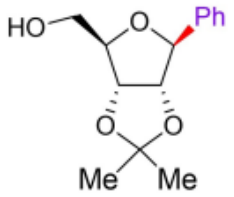

41
72% yield, β

From 5-deoxy-D-ribose

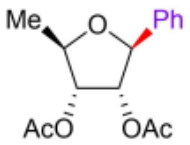

42
65% yield, β

Stereodivergent *C*-aryl glycosylation

a. Possible rationale for difference in stereochemical outcome in glycosyl radical arylation

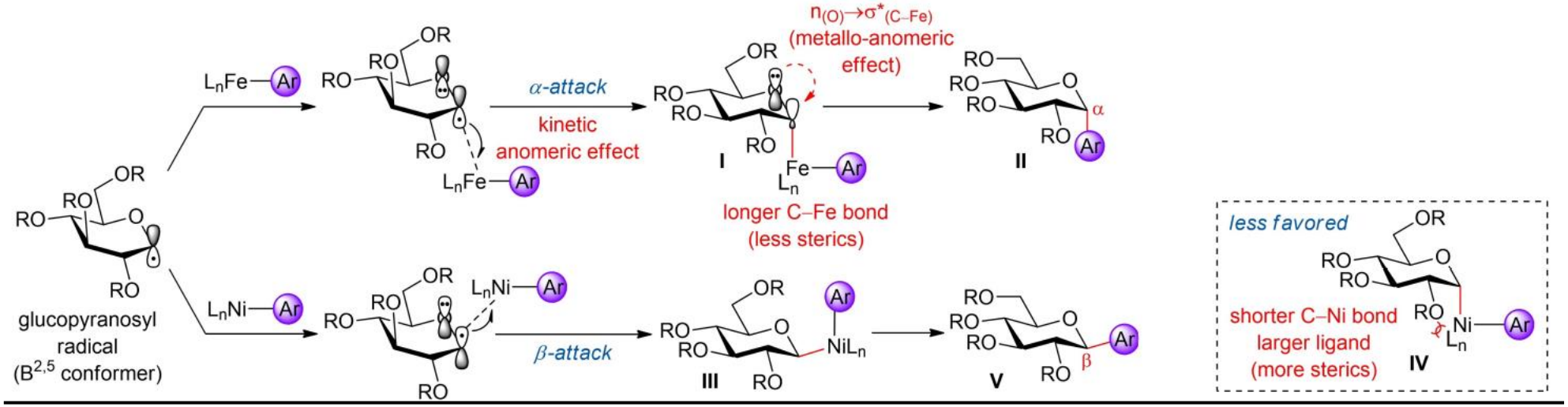

b. Stereodivergent arylation for representative sugar residues

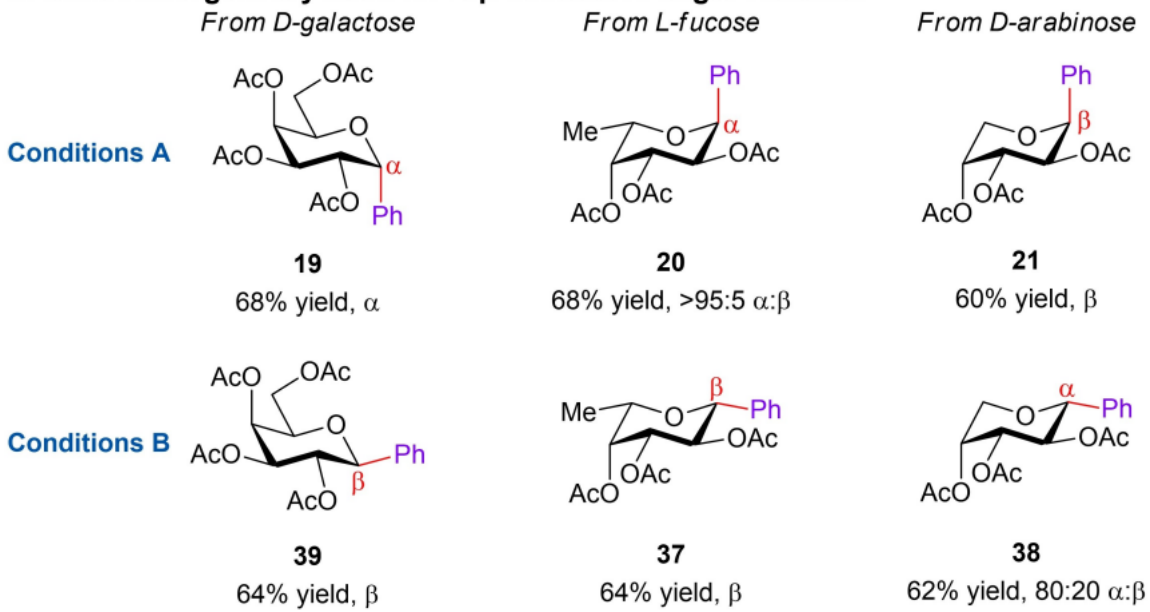

Q. Wang, *et al. Angew. Chem. Int. Ed*. **2023**, *62,* e202301081.
A. G. Orpen, *et al. J. Chem. Soc. Dalton Trans.* **1989**, S1–S83.

Outline

1. Introduction

2. Contents

    2-1. Homolytic activation of hydroxyl group and formation of radicals

    2-2. Stereoselective *C*-aryl glycosylation by catalytic cross-coupling of heteroaryl glycosyl sulfones

    2-3. Direct synthesis of unprotected aryl *C*-glycosides by photoredox Ni-catalysed cross-coupling

3. Summary

Direct synthesis of aryl *C*-glycosides by photoredox Ni-catalysed cross-coupling

a. Classical routes to aryl C-glycosides that use protected intermediates

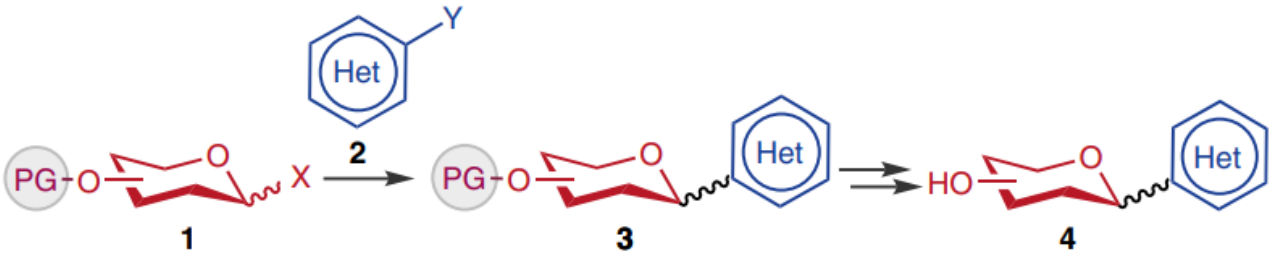

X	Y
Hal	Mg^*/Zn^*
$SnBu_3/BF_3$	Hal
Hal	Hal

Challenges:

- PG removal after glycosidic bond forming
- Unstable starting materials
- Stereoselectivity control

Takeda, D. *et al. Org. Lett,* **2021**, *23,* 1940–1944.
Liu, J., Lei, C., Gong, H. *Sci. China Chem,* **2019**, *62*, 1492–1496.

b. Direct, stereoselective synthesis of unprotected aryl C-glycosides

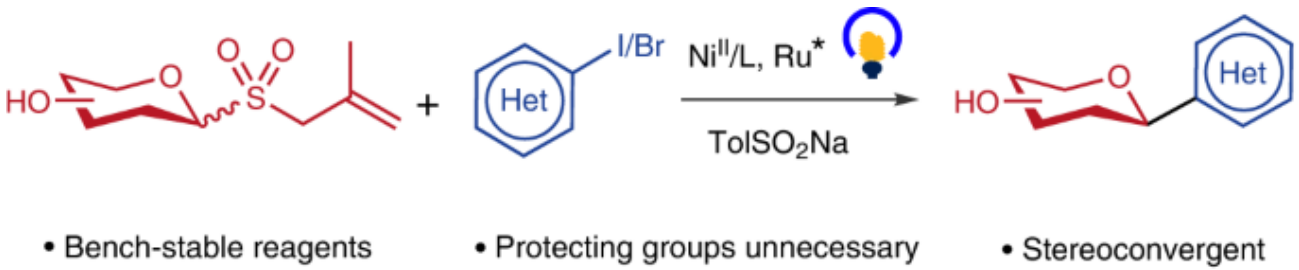

- Bench-stable reagents
- Protecting groups unnecessary
- Stereoconvergent

Representative products:

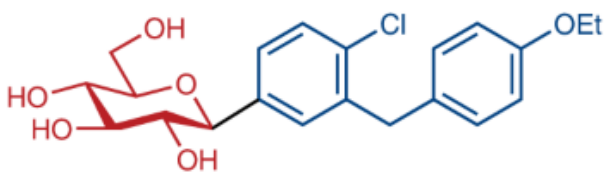

Dapagliflozin

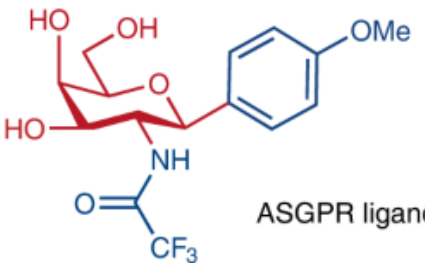

ASGPR ligand

Zhang, C., Xu, SY., Zuo, H. *et al. Nat. Synth,* **2023,** *2*, 251–260.

Mechanistic studies

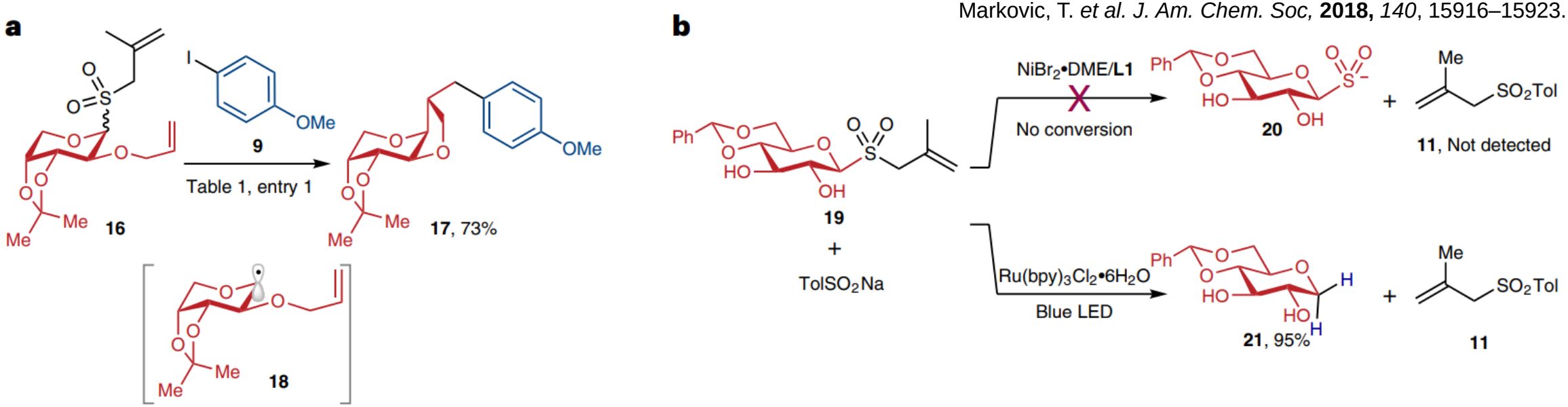

Markovic, T. *et al. J. Am. Chem. Soc,* **2018,** *140*, 15916–15923.

a.

The trap of the allyl group in **16** to form a tetrahydrofuran ring in **17** suggests the intermediacy of glycosyl radical **18.**

b.

Glycosyl radicals is triggered by initial generation of a tolyl sulfonyl radical.
→ Tolyl sulfonyl radical subsequently adds to the terminal alkene group of **19**.
(Not a Ni-catalyzed allylic substitution process.)

Zhang, C., Xu, SY., Zuo, H. *et al. Nat. Synth,* **2023,** *2*, 251–260.

Proposed mechanism

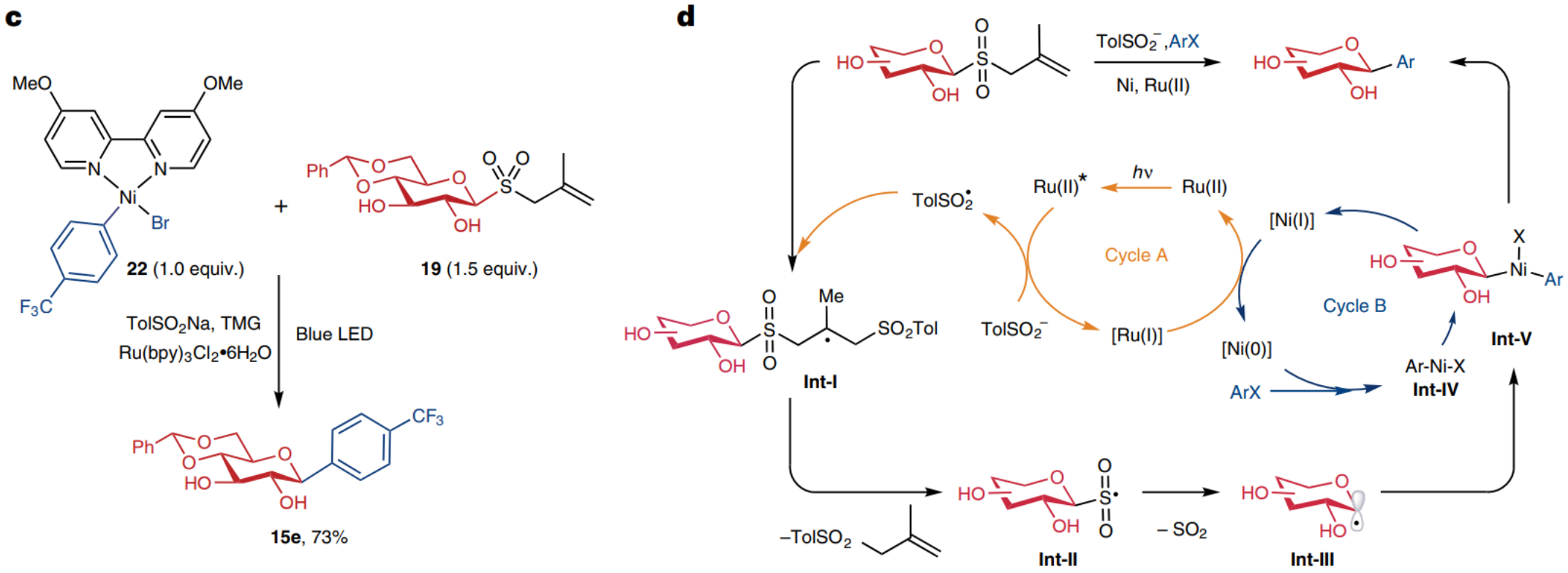

c.

Product **15e** was formed in excellent yield and stereoselectivity, supporting the intermediacy of **22**.

d.

An alternative pathway involving glycosyl radical addition to Ni(0) could be operating as well.

Gutierrez, O. et al. *J. Am. Chem. Soc,* **2015,** *137,* 4896–4899.
Zhang, C., Xu, SY., Zuo, H. *et al. Nat. Synth,* **2023,** *2*, 251–260.

Condition optimization

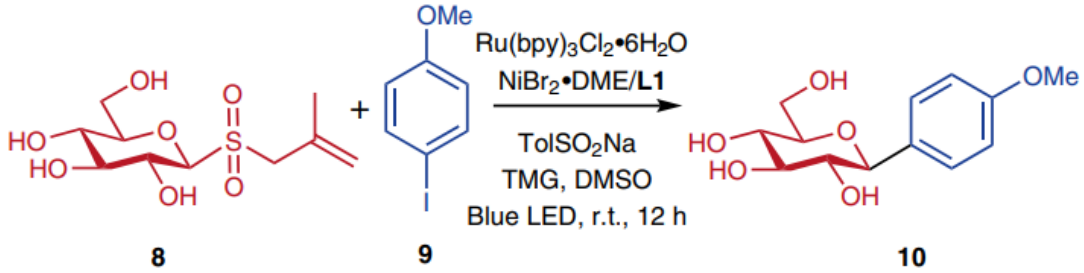

Entry	Deviation from standard conditions	Yield of **10**	β:α
1	None	86%	>19:1
2	Without Ru(II) or $TolSO_2Na$	<5%	ND
3	Without Ni(II) or **L1** or TMG	<5%	ND
4	*fac*-Ir(ppy)$_3$ instead of Ru(II)	<5%	ND
5	4-CzIPN instead of Ru(II)	23%	>19:1
6	DBU instead of TMG	15%	>19:1
7	**L2** instead of **L1**	<5%	ND
8	CF_3SO_2Na instead of $TolSO_2Na$	<5%	ND
9	Pyridine-2-thiol instead of $TolSO_2Na$	<5%	ND
10	MeCN as solvent	8%	ND
11	DMA as solvent	74%	>19:1
12	DMF as solvent	85%	>19:1

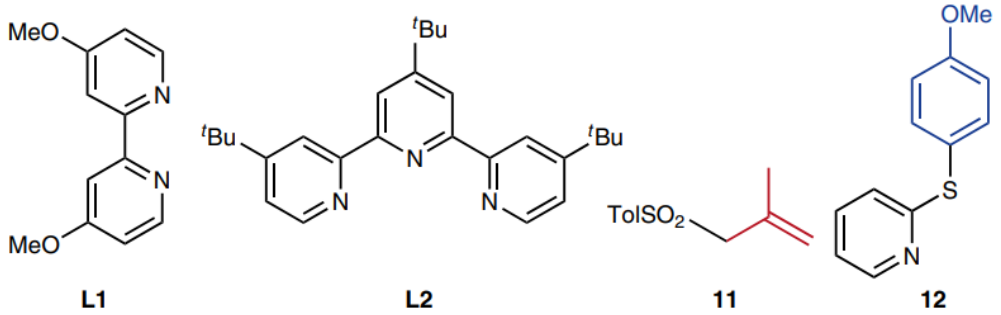

- The potentially competing reactions was not observed.

(a) C–O coupling between the free hydroxyl groups in **8** with **9**

Terrett, J. A. *et al. Nature,* **2015**, *524,* 330–334.
MacQueen, P. M. *et al. J. Am. Chem. Soc,* **2018,** *140*, 5023–5027.

(b) C–S coupling between $TolSO_2Na$ with **9**

Cabrera-Afonso, M. *et al. Chem. Sci,* **2018**, *9,* 3186–3191.

- The direct C–S coupling with **9** to form **12** became the dominant process using pyridine-2-thiol instead of $TolSO_2Na$ (entry9).

Zhang, C., Xu, SY., Zuo, H. *et al. Nat. Synth,* **2023,** *2*, 251–260.

Substrate scope of aryl halides

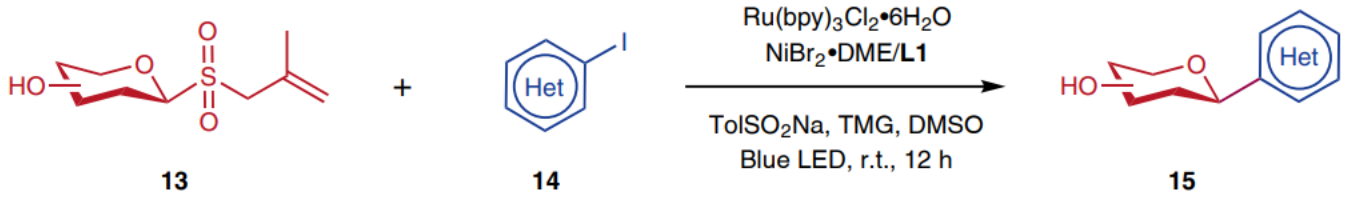

Scope of aryl halides[a]

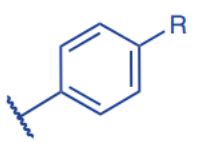

	R	Yield	β:α
15a	OMe	86%	>19:1
15b	Me	58%	>19:1
15c	OCF_3	50%	>19:1
15d	^{t}Bu	46%	>19:1
15e	CF_3	60%[b]	>19:1

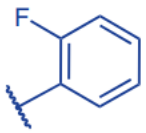

15f, 53%
β:α > 19:1

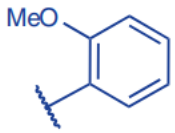

15g, 51%
β:α > 19:1

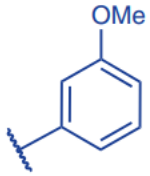

15h, 85%
β:α > 19:1

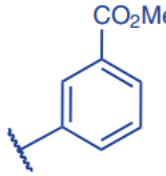

15i, 60%[b]
β:α > 19:1

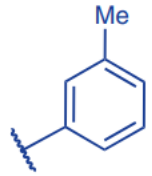

15j, 73%
β:α > 19:1

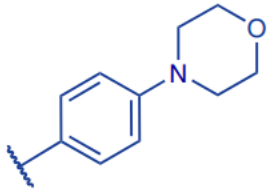

15k, 65%
β:α > 19:1

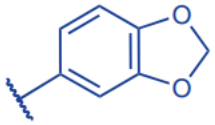

15l, 94%
β:α > 19:1

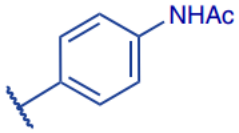

15m, 70%
β:α > 19:1

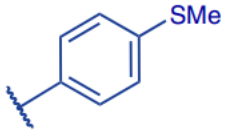

15n, 52%
β:α > 19:1

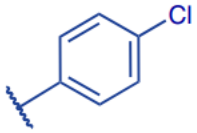

15o, 57%
β:α > 19:1

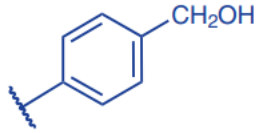

15p, 42%
β:α > 19:1

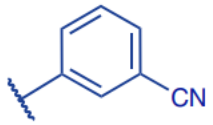

15q, 51%
β:α = 8:1

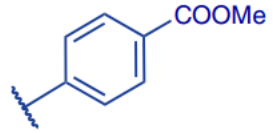

15r, 61%[b]
β:α = 10:1

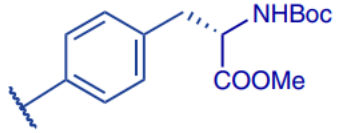

15s, 75%
β:α > 19:1

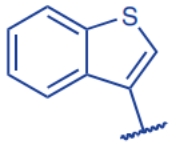

15t, 79%
β:α > 19:1

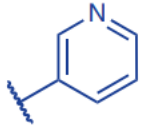

15u, 53%[b]
β:α = 10:1

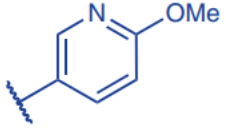

15v, 87%[b]
β:α = 13:1

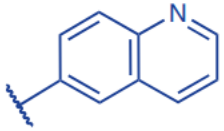

15w, 50%[b]
β:α = 15:1

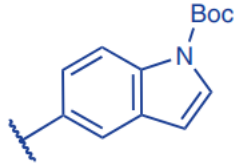

15x, 79%
β:α > 19:1

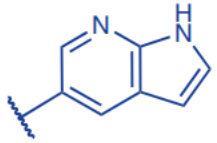

15y, 91%[b]
β:α = 8:1

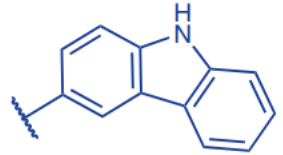

15z, 72%
β:α = 9:1

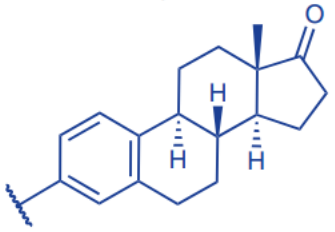

15aa, 77%[c]
β:α > 19:1

Zhang, C., Xu, SY., Zuo, H. *et al. Nat. Synth,* **2023,** *2*, 251–260.

Substrate scope of glycosyl donor

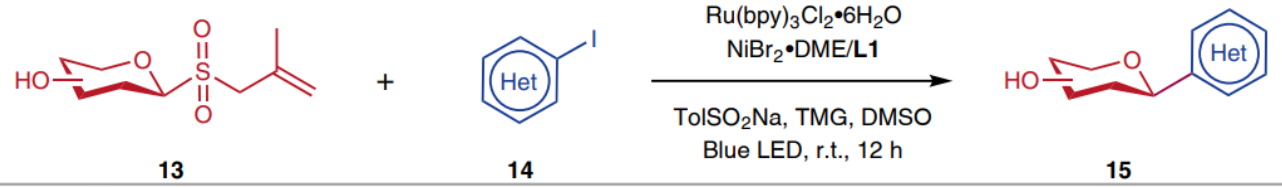

Scope of glycosyl donor

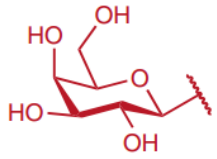

(From galactose)
15ac, 81%
β:α > 19:1

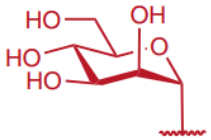

(From mannose)
15ad, 61%[b]
α:β = 6:1

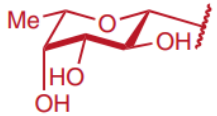

(From fucose)
15ae, 88%[b]
β:α > 19:1

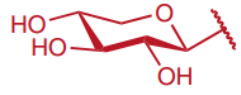

(From xylopyranose)
15af, 77%[b]
β:α > 19:1

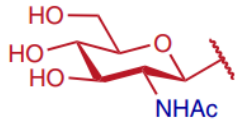

(From 2-glucosamine)
15ag, 77%
β:α > 19:1

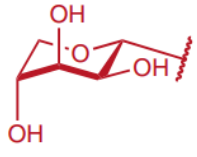

(From lyxose)
15ah, 79%[b]
α:β = 4:1

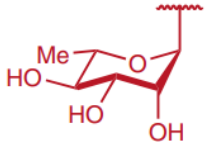

(From rhamnose)
15ai, 70%[b]
α:β = 2.5:1

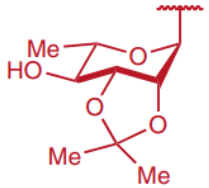

(From rhamnose)
15aj, 87%
α:β = 7:1

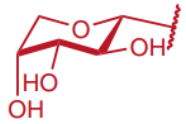

(From arabinose)
15ak, 80%[b]
α:β > 19:1

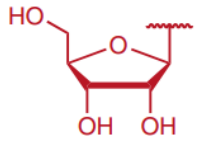

(From ribose)
15al, 76%[b]
β:α = 5:1

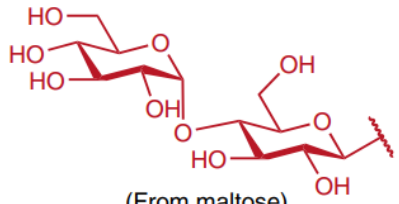

(From maltose)
15am, 81%
β:α = 9:1

Synthesis of glycoconjugates

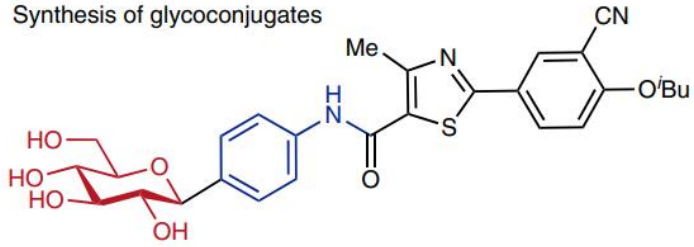

15an, 82%, β:α > 19:1
Febuxostat-glucose conjugate

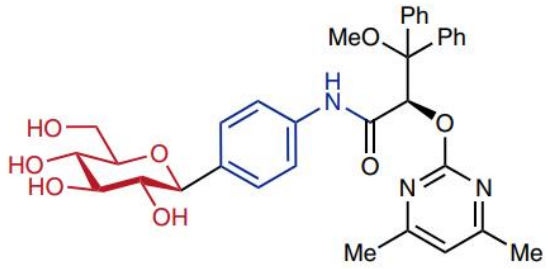

15ao, 78%, β:α > 19:1
Ambrisentan-glucose conjugate

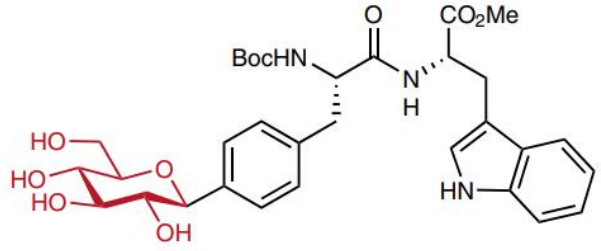

15ap, 65%, β:α > 19:1
TyrTrp-glucose conjugate

Zhang, C., Xu, SY., Zuo, H. *et al. Nat. Synth,* **2023,** *2*, 251–260.

Computed pathway of the reaction between glucopyranosyl radical and OA complex

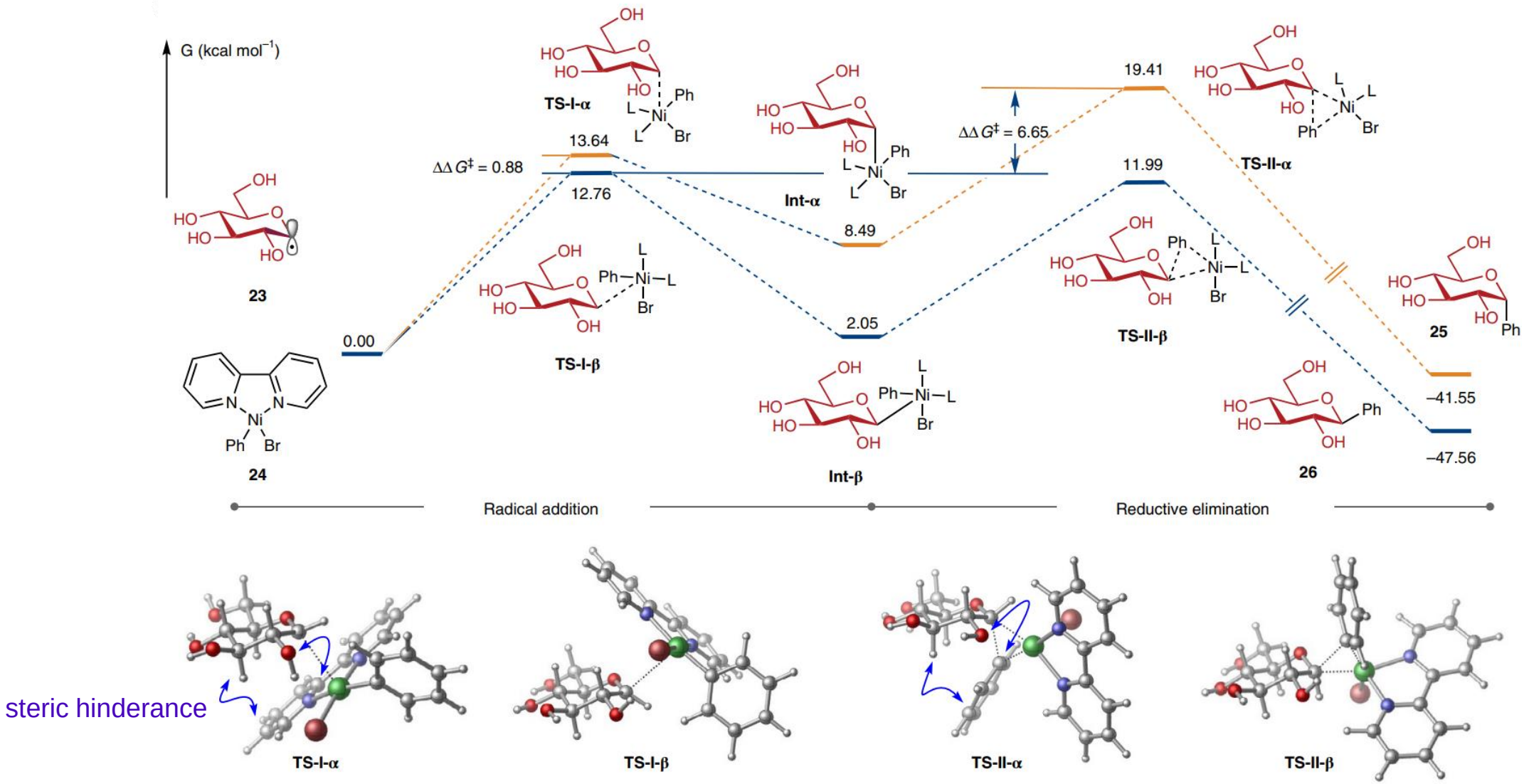

The ligated metal unit clashes with both the sugar ring system and the C2-hydroxyl group.

Zhang, C., Xu, SY., Zuo, H. *et al. Nat. Synth,* **2023,** *2*, 251–260.

Comparing the activation free energies of reactions

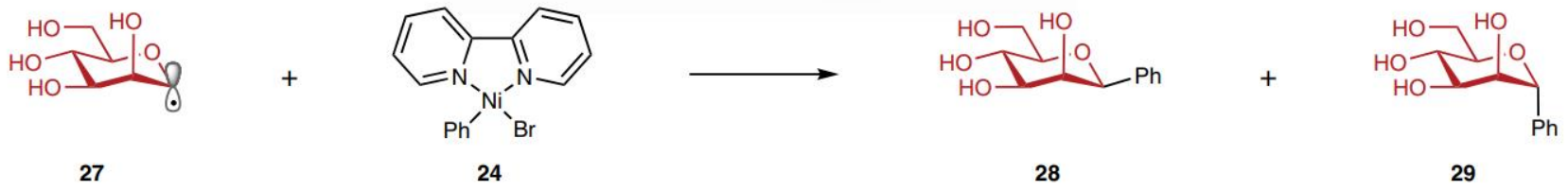

steric hinderance

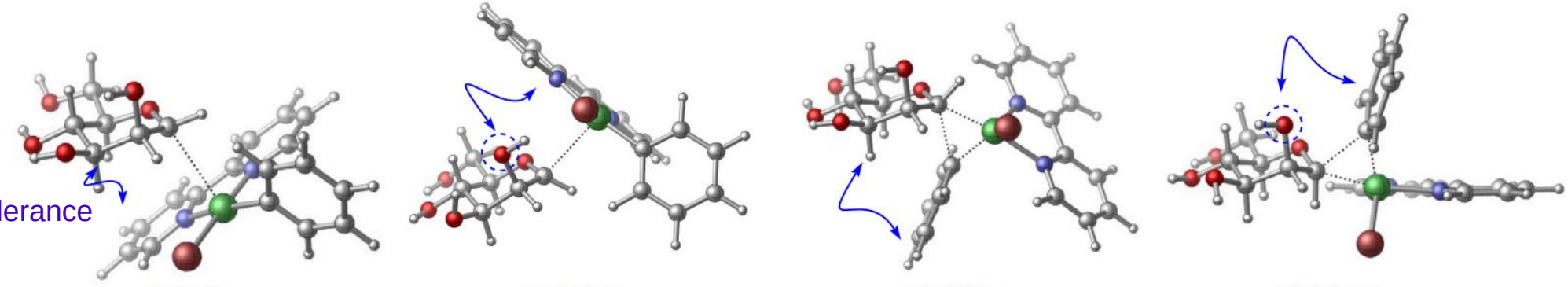

ManTS-I-α
14.86 kcal mol^{-1}

ManTS-I-β
14.54 kcal mol^{-1}

ManTS-II-α
14.15 kcal mol^{-1}

ManTS-II-β
14.74 kcal mol^{-1}

	$\Delta G^{\ddagger}$ of radical addition	$\Delta G^{\ddagger}$ of reductive elimination
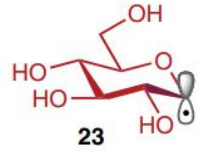 **23**	12.76 kcal mol^{-1}	11.99 kcal mol^{-1}
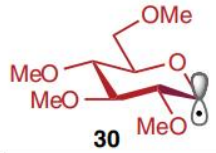 **30**	20.31 kcal mol^{-1}	15.17 kcal mol^{-1}

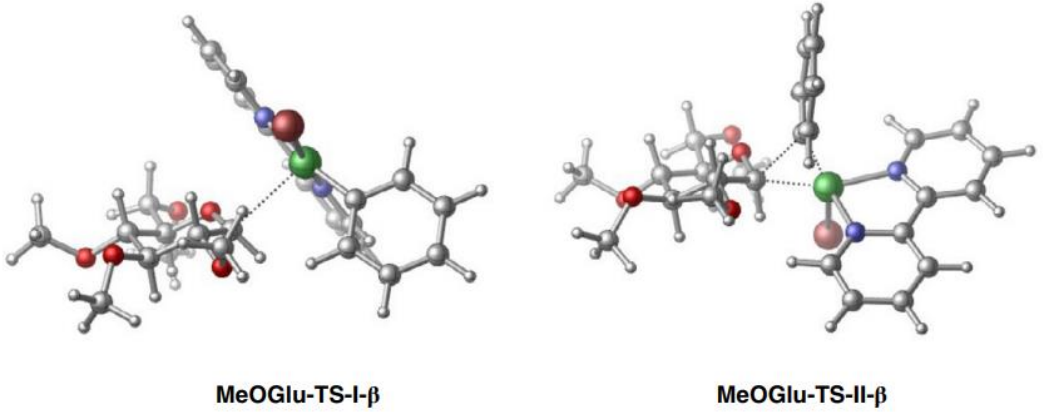

MeOGlu-TS-I-β

MeOGlu-TS-II-β

The radical addition using protected radical to the OA complex becomes considerably more difficult.

Zhang, C., Xu, SY., Zuo, H. *et al. Nat. Synth,* **2023,** *2*, 251–260.

Conformational stability of protected and unprotected glucosyl radicals

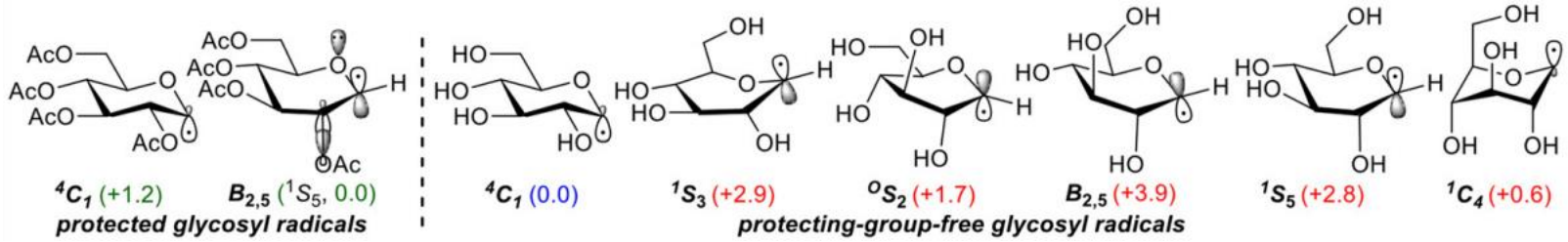

- The most stable conformation for the tetraacetyl glucosyl radical is $B_{2,5}$ (or $^1S_5$) conformation.
- The most stable conformation for the protecting-group-free glucosyl radical is $^4C_1$ conformation.

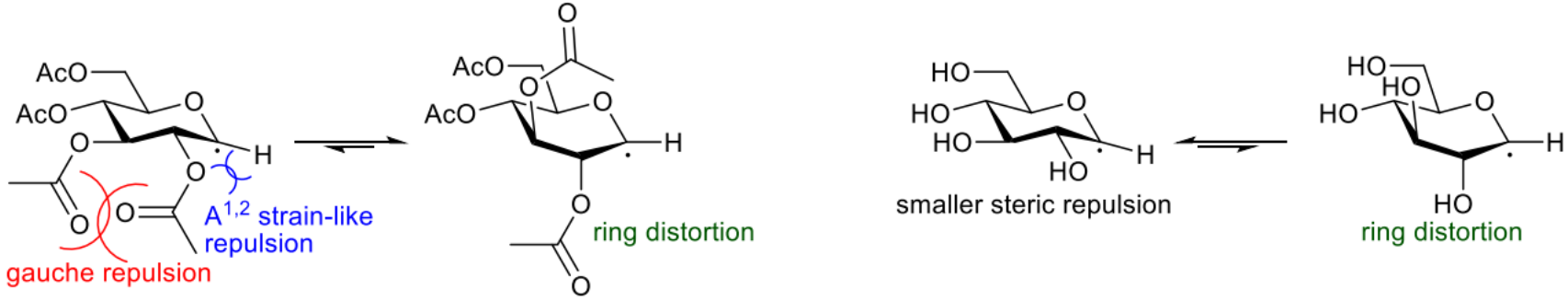

- The 2-OP and 3-OP groups of the protected glucosyl radical adopt a pseudo-axial position to reduce steric repulsion, resulting in the formation of the $B_{2,5}$ conformation.

- Steric factors are negligible in the unprotected glucosyl radical, leading to the preferable existence of the $^4C_1$ conformation.

T. Miura, *et al. Chem. Commun*, **2023**, *59*, 8564.
H. Abe, S. Shuto, A. Matsuda, *J. Am. Chem. Soc*. **2001**, *123*, 11870.

Outline

1. Introduction

2. Contents

    2-1. Homolytic activation of hydroxyl group and formation of radicals

    2-2. Stereoselective C-aryl glycosylation by catalytic cross-coupling of heteroaryl glycosyl sulfones

    2-3. Direct synthesis of unprotected aryl C-glycosides by photoredox Ni-catalysed cross-coupling

3. Summary

Summary

Synthesis of Aryl *C*-Glycosides via Radical Pathway

- ✓ Independence on the structures of donors.
- ✓ Mild conditions.
- ✓ Functional group tolerant.

2-2. Stereoselective *C*-aryl glycosylation by catalytic cross-coupling of heteroaryl glycosyl sulfones

- ✓ Bench-stable and easily accessible donors.
- ✓ Distinct mechanisms and activation modes.
- ✓ Access to both α and β isomers for key sugars.

2-3. Direct synthesis of unprotected aryl *C*-glycosides by photoredox Ni-catalysed cross-coupling

- ✓ Stereoconvergent, diastereoselective
- ✓ Protecting groups unnecessary
- ✓ Bench-stable and easily accessible donors

Appendix: Aryl C-glycosides

(a) Previously reported method

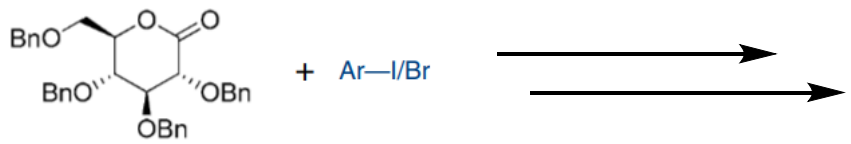

× Three steps × Harsh conditions

(b) New method via glycosyl radical

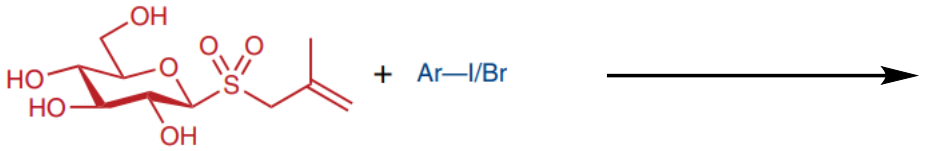

✓ One step ✓ Mild conditions

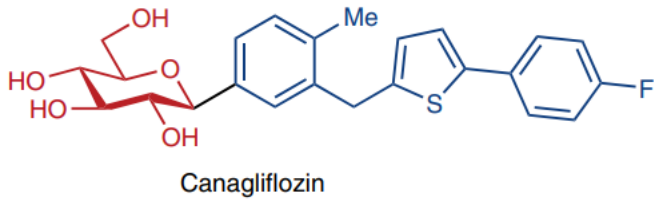

SGLT2 inhibitors against type Ⅱ diabetes

Chao, E. C.; Henry, R. R. *Nat. Rev. Drug Discovery* **2010**, *9*, 551−559.
(a) Aguillón, A. R. et al. *Org. Proc. Res. Dev*. **2018,** *22*, 467–488.
(b) Zhang, C., Xu, SY., Zuo, H. *et al. Nat. Synth,* **2023,** *2*, 251–260.

Appendix : Optimization of the coupling reaction

Entry	Change	**18** (GC yield)
1	no change	84%
2	**17**(1.0 equiv.)	74%
3	**17**(1.5 equiv.)	88%
4	DMAc instead of 1,4-dioxane	trace
5	DMF instead of 1,4-dioxane	trace
6	tetrahydropyran instead of 1,4-dioxane	78%
7	NaOMe instead of Na_2CO_3	trace
8	NaO^tBu instead of Na_2CO_3	trace
9	$NaHCO_3$ instead of Na_2CO_3	trace
10	LiO^tBu instead of Na_2CO_3	trace
11	**L1** instead of bpy	81%
12	**L2** instead of bpy	69%
13	**L3** instead of bpy	75%
14	without 4CzIPN	0
15	without $NiBr_2$•DME	0
16	Commercial $NiBr_2$•DME	84%
17	$NiCl_2$•DME	82%
18	r.t.	0
19	70 °C instead of 84 °C	66%

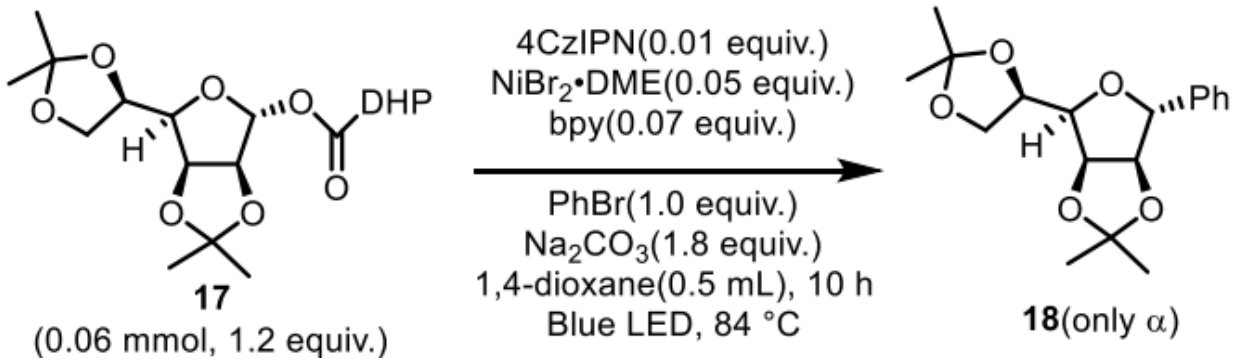

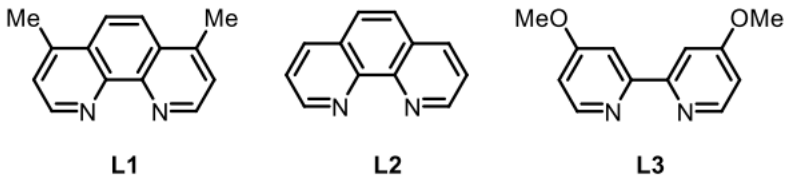

Wei, Y., Ben-Zvi, B., Diao, T. *Angew. Chem. Int. Ed.* **2021**, *60*, 9433.

Appendix: Extended reaction scopes of 2-2

Fe-catalyzed desulfonylative arylation

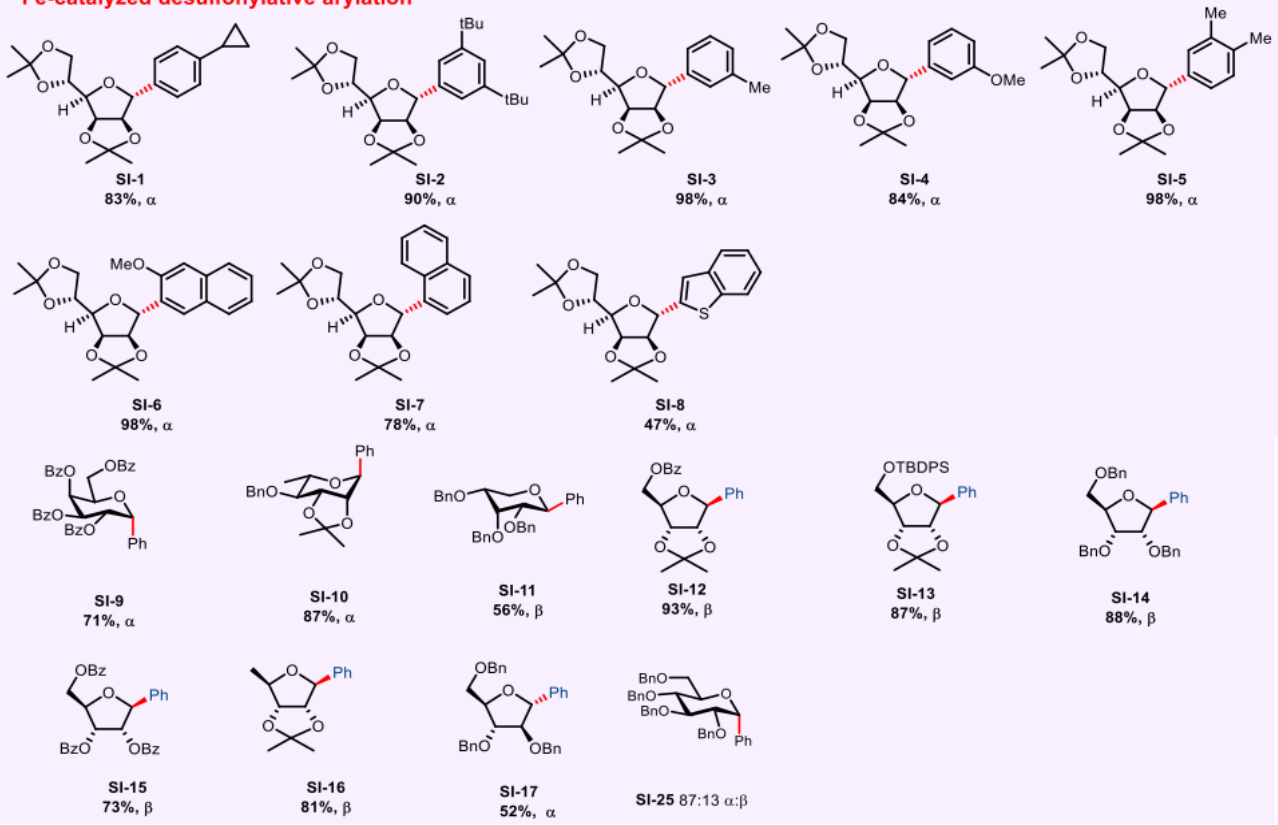

Ni-catalyzed desulfonylative arylation

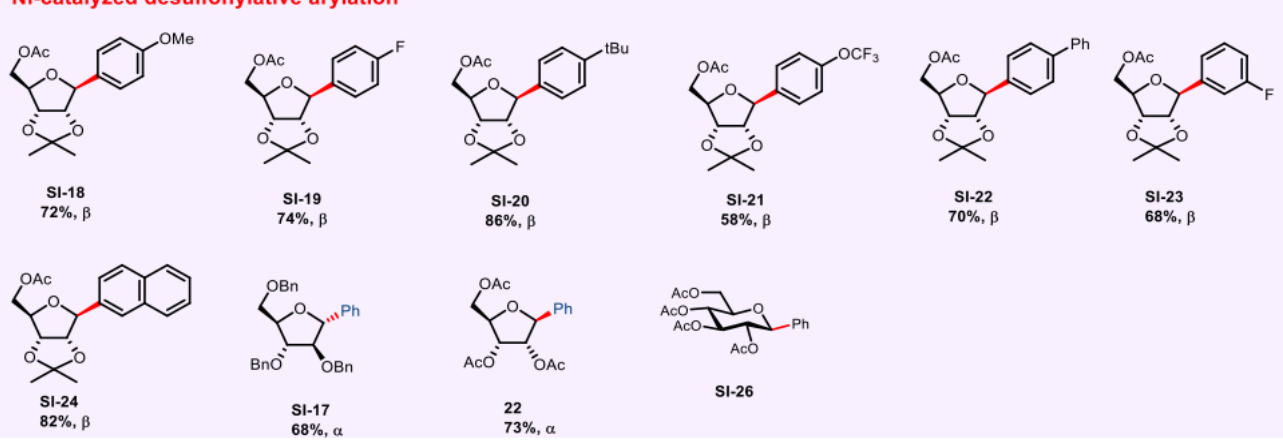

Q. Wang, *et al. Angew. Chem. Int. Ed*. **2023**, *62,* e202301081.

Appendix: Screen of photocatalyst and ligands

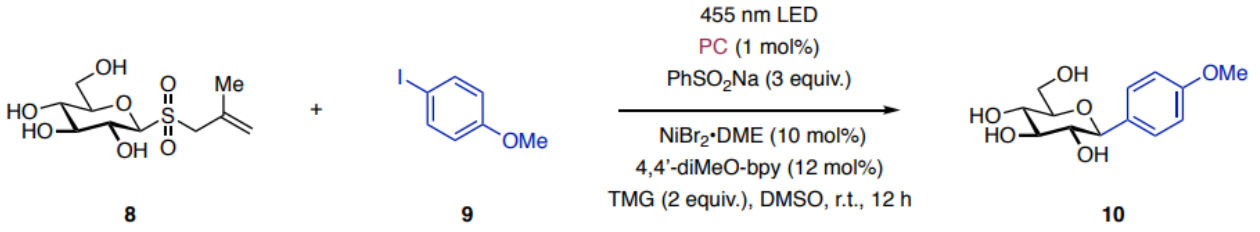

Entry	PC	Yield (%)
1	PC-1: $Ru(bpy)_3Cl_2•6H_2O$	59
2	PC-2: $Ru(1,10\text{-}Phen)_3[PF_6]_2$	42
3	PC-3: $Ru(bpz)_3[PF_6]_2$	0
4	PC-4: *fac*-Ir(ppy)$_3$	0
5	PC-5: 4-CzIPN	23
6	PC-6: Mes-Acr$^+$ ClO_4^-	0

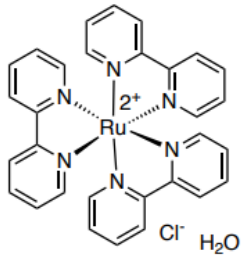

PC-1: $Ru(bpy)_3Cl_2•6H_2O$

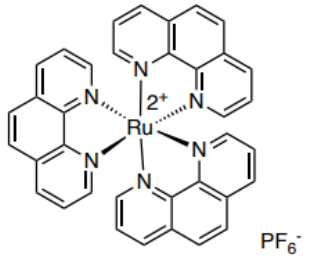

PC-2: $Ru(1,10\text{-}Phen)_3[PF_6]_2$

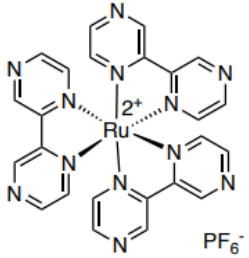

PC-3: $Ru(bpz)_3[PF_6]_2$

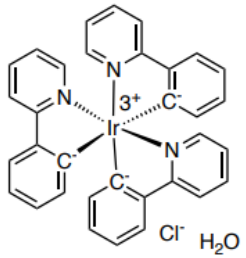

PC-4: $Ru(bpy)_3Cl_2•6H_2O$

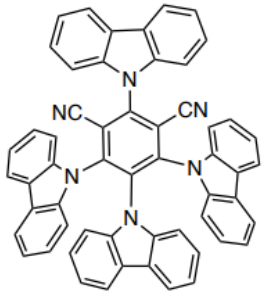

PC: 4-CzIPN

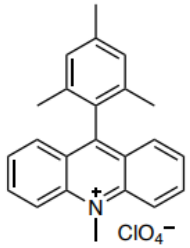

PC-6: Mes-Acr$^+$ ClO_4^-

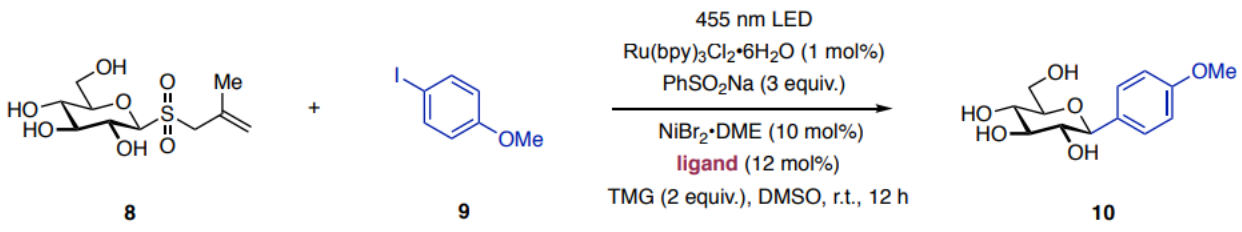

Entry	ligand	Yield (%)
1	L-1	63
2	L-2	59
3	L-3	56
4	L-4	29
5	L-5	55
6	L-6	56

Entry	ligand	Yield (%)
1	L-7	19
2	L-8	47
3	L-9	51
4	L-10	29
5	L-11	0
6	L-12	0

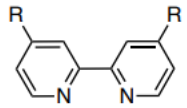

L-1, R = OMe
L-2, R = Me
L-3, R = *t*-Bu
L-4, R = COOMe
L-5, R = H

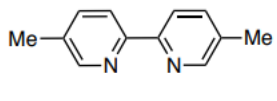

L-6

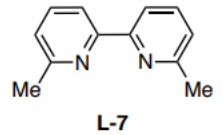

L-7

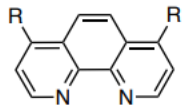

L-8, R = H
L-9, R = Ph

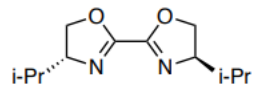

L-10

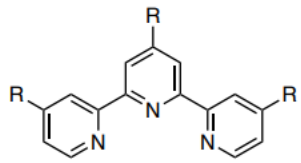

L-11, R = H; **L-12**, R = *t*-Bu

Zhang, C., Xu, SY., Zuo, H. *et al. Nat. Synth,* **2023,** *2*, 251–260.

Appendix: Screen of nickel catalysts and solvents

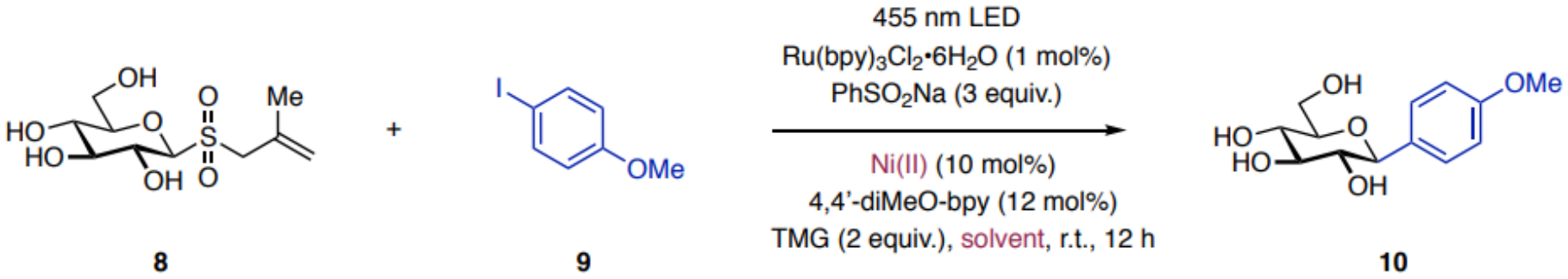

Entry	Ni(II) (DMSO as solvent)	Yield (%)	Entry	Solvent ($NiBr_2$•DME as catalyst)	Yield (%)
1	$NiCl_2$	55	6	MeCN	8
2	$Ni(OAc)_2$	49	7	EtOAc	0
3	$Ni(AcAc)_2$	0	8	H_2O	0
4	$Ni(OTf)_2$	0	9	DMA	74
5	$Ni(PPh_3)_2Cl_2$	47	10	DMF	85

Zhang, C., Xu, SY., Zuo, H. *et al. Nat. Synth,* **2023,** *2*, 251–260.

Appendix: Screen of RSO_2Na additive

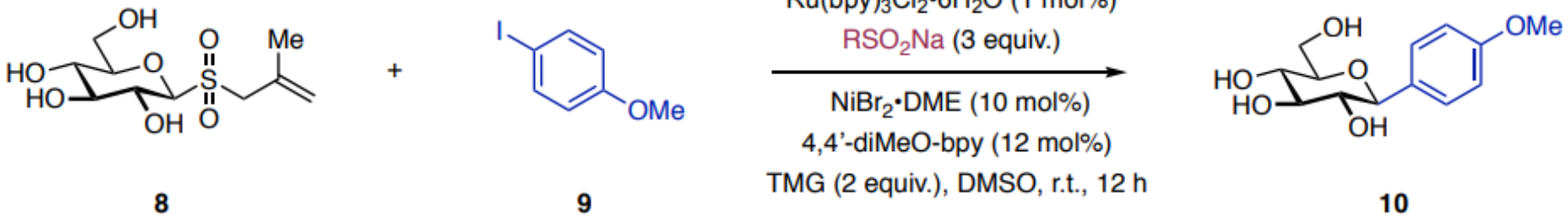

Entry	RSO_2Na	Yield (%)	Entry	RSO_2Na	Yield (%)
1	$PhSO_2Na$	61	5	Cyclopropyl-SO_2Na	55
2	CH_3SO_2Na	49	6	4-Me-$PhSO_2Na$	86
3	CF_3SO_2Na	0	7	4-F-$PhSO_2Na$	61
4	$EtSO_2Na$	51	8	4-Cl-$PhSO_2Na$	70

Zhang, C., Xu, SY., Zuo, H. *et al. Nat. Synth,* **2023,** *2*, 251–260.

Appendix: Synthetic applications

a.

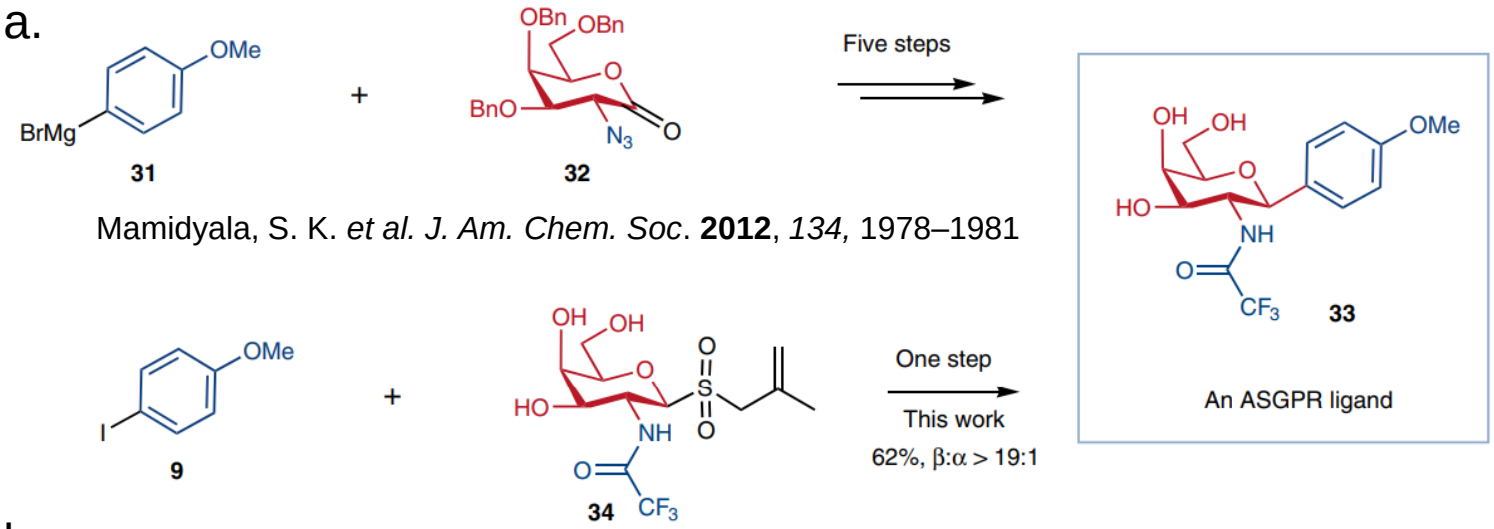

Mamidyala, S. K. *et al. J. Am. Chem. Soc*. **2012**, *134,* 1978–1981

b.

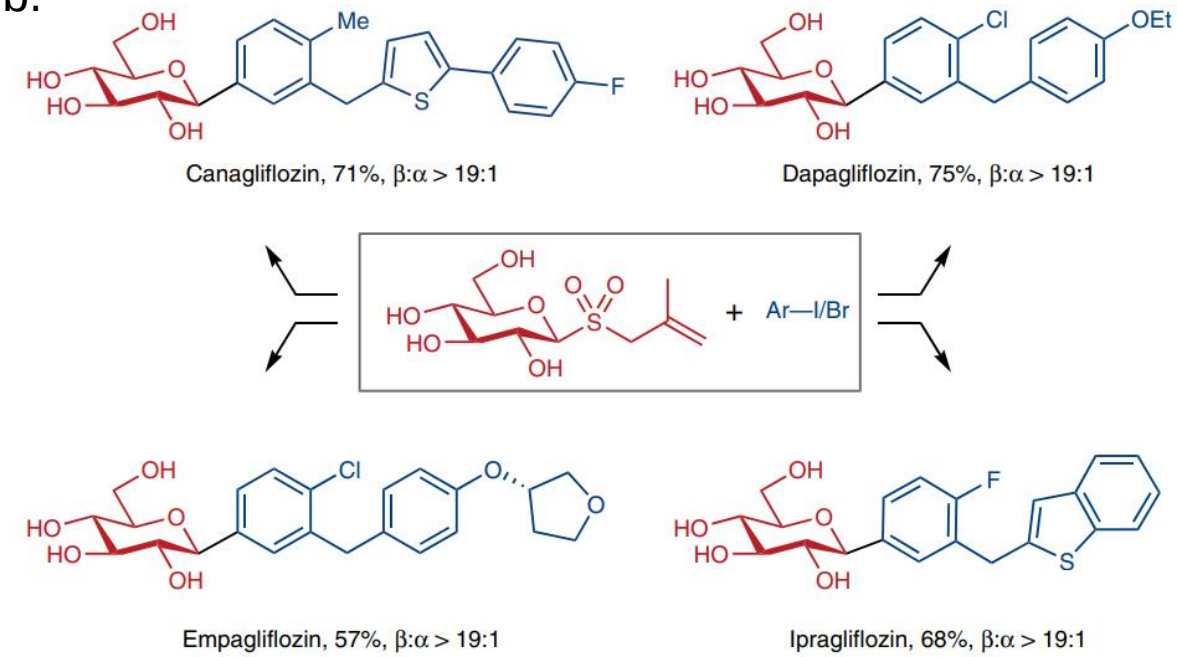

a. Synthesis of ASGPR ligand by literature methods compared with this work.

b. Synthesis of gliflozins.

Aguillón, A. R. et al. *Org. Proc. Res. Dev*. **2018,** *22*, 467–488.
Zhang, C., Xu, SY., Zuo, H. *et al. Nat. Synth,* **2023,** *2*, 251–260.

Appendix: Relative free energies of intermediates and transition structures

conformer / G (kcal/mol) / Intermediates/TS	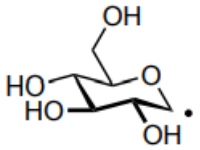 $^4C_1$-Glu Radical	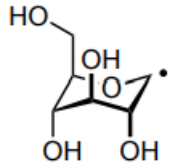 $^1C_4$-Glu Radical	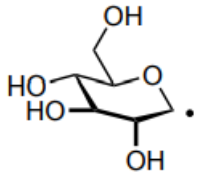 $B_{2,5}$-Glu Radical
Glycosyl Radical:	0	4.69	1.94
TS-I-α (radical addition):	13.64	19.01	16.02
TS-I-β (radical addition):	12.76	23.32	23.15
Ni(III)-Int-α:	8.49	9.76	10.32
Ni(III)-Int-β:	2.05	15.08	15.81
TS-II-α (reductive elimination):	19.41	17.89	23.43
TS-II-β (reductive elimination):	11.99	22.44	15.78

conformer / G (kcal/mol) / Intermediates/TS	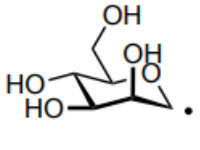 $^4C_1$-Man Radical	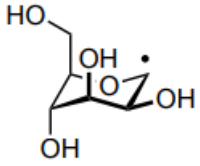 $^1C_4$-Man Radical	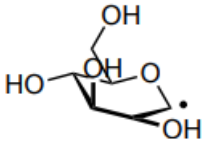 $B_{2,5}$-Man Radical
Glycosyl Radical:	0	9.39	5.65
TS-I-α (radical addition):	14.86	24.46	24.70[a]
TS-I-β (radical addition):	14.54	27.44	24.89
Ni(III)-Int-α:	7.25	14.02	12.01
Ni(III)-Int-β:	9.06	23.68	19.35
TS-II-α (reductive elimination):	14.15	24.43	24.51
TS-II-β (reductive elimination):	14.74	22.65	28.08

Zhang, C., Xu, SY., Zuo, H. *et al. Nat. Synth,* **2023,** *2*, 251–260.